UNIVERSITÀ DI SIENA 1240

dedica a ...

Abstract

Lorem ipsum dolor sit amet, consectetuer adipiscing elit. Ut purus elit, vestibulum ut, placerat ac, adipiscing vitae, felis. Curabitur dictum gravida mauris. Nam arcu libero, nonummy eget, consectetuer id, vulputate a, magna. Donec vehicula augue eu neque. Pellentesque habitant morbi tristique senectus et netus et malesuada fames ac turpis egestas. Mauris ut leo. Cras viverra metus rhoncus sem. Nulla et lectus vestibulum urna fringilla ultrices. Phasellus eu tellus sit amet tortor gravida placerat. Integer sapien est, iaculis in, pretium quis, viverra ac, nunc. Praesent eget sem vel leo ultrices bibendum. Aenean faucibus. Morbi dolor nulla, malesuada eu, pulvinar at, mollis ac, nulla. Curabitur auctor semper nulla. Donec varius orci eget risus. Duis nibh mi, congue eu, accumsan eleifend, sagittis quis, diam. Duis eget orci sit amet orci dignissim rutrum.

Nam dui ligula, fringilla a, euismod sodales, sollicitudin vel, wisi. Morbi auctor lorem non justo. Nam lacus libero, pretium at, lobortis vitae, ultricies et, tellus. Donec aliquet, tortor sed accumsan bibendum, erat ligula aliquet magna, vitae ornare odio metus a mi. Morbi ac orci et nisl hendrerit mollis. Suspendisse ut massa. Cras nec ante. Pellentesque a nulla. Cum sociis natoque penatibus et magnis dis parturient montes, nascetur ridiculus mus. Aliquam tincidunt urna. Nulla ullamcorper vestibulum turpis. Pellentesque cursus luctus mauris.

Ringraziamenti

Lorem ipsum dolor sit amet, consectetuer adipiscing elit. Ut purus elit, vestibulum ut, placerat ac, adipiscing vitae, felis. Curabitur dictum gravida mauris. Nam arcu libero, nonummy eget, consectetuer id, vulputate a, magna. Donec vehicula augue eu neque. Pellentesque habitant morbi tristique senectus et netus et malesuada fames ac turpis egestas. Mauris ut leo. Cras viverra metus rhoncus sem. Nulla et lectus vestibulum urna fringilla ultrices. Phasellus eu tellus sit amet tortor gravida placerat. Integer sapien est, iaculis in, pretium quis, viverra ac, nunc. Praesent eget sem vel leo ultrices bibendum. Aenean faucibus. Morbi dolor nulla, malesuada eu, pulvinar at, mollis ac, nulla. Curabitur auctor semper nulla. Donec varius orci eget risus. Duis nibh mi, congue eu, accumsan eleifend, sagittis quis, diam. Duis eget orci sit amet orci dignissim rutrum.

Nam dui ligula, fringilla a, euismod sodales, sollicitudin vel, wisi. Morbi auctor lorem non justo. Nam lacus libero, pretium at, lobortis vitae, ultricies et, tellus. Donec aliquet, tortor sed accumsan bibendum, erat ligula aliquet magna, vitae ornare odio metus a mi. Morbi ac orci et nisl hendrerit mollis. Suspendisse ut massa. Cras nec ante. Pellentesque a nulla. Cum sociis natoque penatibus et magnis dis parturient montes, nascetur ridiculus mus. Aliquam tincidunt urna. Nulla ullamcorper vestibulum turpis. Pellentesque cursus luctus mauris.

Contents

Introduction

Lorem ipsum dolor sit amet, consectetuer adipiscing elit. Ut purus elit, vestibulum ut, placerat ac, adipiscing vitae, felis. Curabitur dictum gravida mauris. Nam arcu libero, nonummy eget, consectetuer id, vulputate a, magna. Donec vehicula augue eu neque. Pellentesque habitant morbi tristique senectus et netus et malesuada fames ac turpis egestas. Mauris ut leo. Cras viverra metus rhoncus sem. Nulla et lectus vestibulum urna fringilla ultrices. Phasellus eu tellus sit amet tortor gravida placerat. Integer sapien est, iaculis in, pretium quis, viverra ac, nunc. Praesent eget sem vel leo ultrices bibendum. Aenean faucibus. Morbi dolor nulla, malesuada eu, pulvinar at, mollis ac, nulla. Curabitur auctor semper nulla. Donec varius orci eget risus. Duis nibh mi, congue eu, accumsan eleifend, sagittis quis, diam. Duis eget orci sit amet orci dignissim rutrum.

Nam dui ligula, fringilla a, euismod sodales, sollicitudin vel, wisi. Morbi auctor lorem non justo. Nam lacus libero, pretium at, lobortis vitae, ultricies et, tellus. Donec aliquet, tortor sed accumsan bibendum, erat ligula aliquet magna, vitae ornare odio metus a mi. Morbi ac orci et nisl hendrerit mollis. Suspendisse ut massa. Cras nec ante. Pellentesque a nulla. Cum sociis natoque penatibus et magnis dis parturient montes, nascetur ridiculus mus. Aliquam tincidunt urna. Nulla ullamcorper vestibulum turpis. Pellentesque cursus luctus mauris.

Chapter 1

The Standard Model, Higgs Boson and New Scalar Particles

Chapter 2

CMS e LHC

Chapter 3

Monte Carlo event simulation

Chapter 4

Event Reconstruction

Chapter 5

Analysis strategy

5.1 Analysis strategy

5.1.1 Introduction

The analysis strategy for the high mass search with 2016 data in the $W^+W^- \to 2\ell 2\nu$ decay channel is similar to the previous high mass analysis with 2015 data [1], but has several improvements.
In the opposite-flavour $W^+W^- \to e^\pm\mu^\mp 2\nu$ final state four different jets-categories are defined (they were three in [1]): 0-jet, 1-jet, 2-jet-non VBF and VBF. The 2 jet non-VBF category is new with respect to [1]. A same-flavour (SF) $W^+W^- \to e^+e^- 2\nu$ and $W^+W^- \to \mu^+\mu^- 2\nu$ category, has been added in the VBF phase space. Indeed, the VBF selection cuts are sufficiently tight to reduce the otherwise overwhelming Z+jets background to a manageable level.

Whenever we count jets in this analysis we always refer to AK4 jets with $p_T > 30$ GeV.

Events are requested to pass single or double lepton triggers. Leptons should have a mini- mum p_T of 10 (13) GeV for the muon (electron) candidate. One of the two leptons should also have a p_T greater than 25 GeV and two leptons are requested to be well identified and isolated, to reject non-prompt leptons and leptons coming from QCD sources. These selections are in common to all phase spaces, and are detailed in [2].

The main production mode for the Higgs boson production over the all mass spectrum is the gluon-gluon fusion process (ggH). At a center-of-mass energy of 13 TeV the ggH cross section for a Higgs boson mass (m_H) of 125 GeV is 43.92 pb [3], that is almost one order of magnitude larger than the second process in terms of cross section at that mass, VBF, with 3.748 pb [3]. The ggH cross section decreases with m_H but the VBF/ggH cross section ratio increases with the mass, making the VBF production mechanism more and more important as m_H approaches to high values.
The signal samples are interpreted in terms of the EWK singlet model described in Sec ?? below. The Higgs boson width and lineshape is reweighted at generator level according to the parameters defined in the model. The interference effects between the ggH signal, the ggWW background and SM Higgs boson, that are expected to slightly change the lineshape of the signal distribution, have been fully taken

into account, as detailed in Sec. ??. A similar treatment is also applied for the intereference between the VBF high mass signal, the VBF SM Higgs and the quark initiated WW+2 quarks backgrround. The interference between the $W^+W^- \to 2\ell 2\nu$ and $ZZ \to 2\ell 2\nu$ is negligible due to the different phase space characteristic of these processes.

5.1.2 Discriminating variable

The analysis presented in this note is a shape analysis, meaning that after applying selection cuts detailed in Secs .5.2 and 5.3 below, we do not simply count events, but rather we fit a data histogram of a discriminating variable with the sum of signal and background templates, and extract the signal yield from the fit. The variable with the best discriminating value would be the invariant mass of the four lepton, which is not possible to reconstruct in the WW channel due to neutrinos.

In the SM Higgs analysis (HIG-16-042), a shape analysis based on two-dimensional templates of $m_{\ell\ell}$ versus m_T^H in each of the categories is performed, where the transverse mass m_T^H variable is defined as

$$m_T^H = \sqrt{2 p_{\mathrm{T}}^{\ell\ell} E_{\mathrm{T}}^{\mathrm{miss}} (1 - \cos\Delta\phi(\ell\ell, \vec{p}_{\mathrm{T}}^{\mathrm{miss}}))} \tag{5.1}$$

where $\Delta\phi(\ell\ell, \vec{p}_{\mathrm{T}}^{\mathrm{miss}})$ is the azimuthal angle between the dilepton momentum and $\vec{p}_{\mathrm{T}}^{\mathrm{miss}}$.
However m_T^H (and also $m_{\ell\ell}$) is not very sensitive to the signal mass hypothesis, so a *new* variable m_T^I defined as the visible mass,

$$m_T^I = \sqrt{(p_{\ell\ell} + E_{\mathrm{T}}^{\mathrm{miss}})^2 - (\vec{p}_{\ell\ell} + \vec{p}_{\mathrm{T}}^{\mathrm{miss}})^2} \tag{5.2}$$

has been introduced in 2015 analysis to discriminate better the signals generate at different masses. The distribution of the variables defined above are shown in Fig. 5.1, where the better power of m_T^I in discriminating different mass hypotheses over other variable is visible.

5.2 Opposite Flavor final state

In this section the analysis for the opposite-flavour final state $W^+W^- \to \mu^\pm e^\mp 2\nu$ is described.

5.2.1 Signal region

The events are requested to pass single or double lepton triggers, and exactly one electron and one muon are requested to be reconstructed in the event.

One of the two leptons is requested to have a p_T greater than 25 GeV , the other is requested to have p_T greater than 20 GeV and both leptons are requested to be well identified and isolated, to reject non-prompt leptons and leptons coming from QCD sources. To suppress background processes with three or more leptons in the final state, such as ZZ, WZ, $Z\gamma$, $W\gamma$ or triboson production, no additional identified

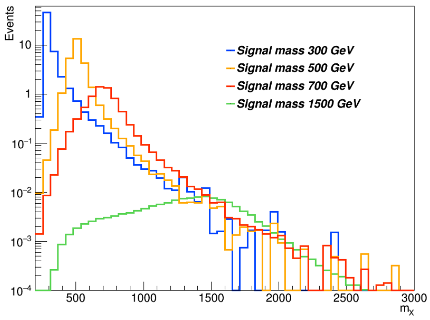

(a) True generated mass

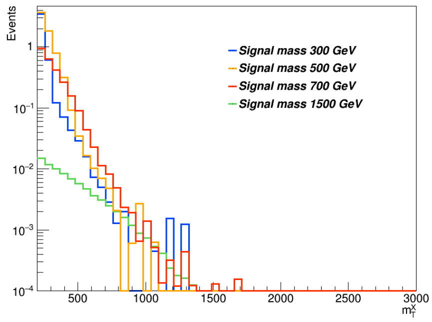

(b) m_T^H

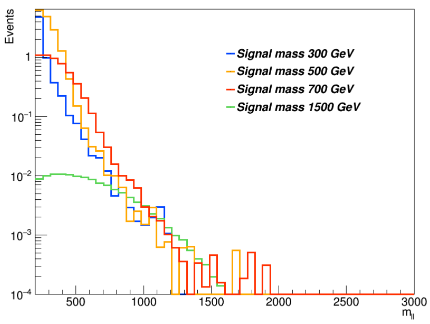

(c) $m_{\ell\ell}$

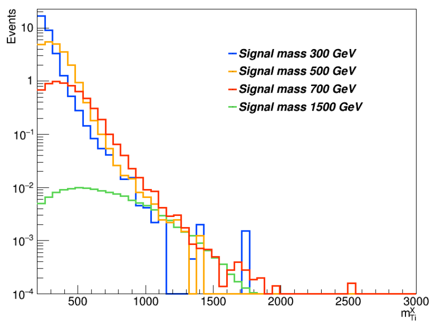

(d) m_T^I

Figure 5.1. Distributions of the generated mass, m_T^H, $m_{\ell\ell}$ and m_T^I variables for different Higgs mass hypothesis, without any selection. The same distribution after the OF selection are shown in Appendix **??**.

and isolated lepton with $p_T > 10$ GeV should be reconstructed. The low dilepton invariant mass region dominated by QCD production of leptons is not considered in the analysis and $m_{\ell\ell}$ is requested to be higher than 50 GeV to reduce the SM Higgs boson (m_H=125 GeV) contamination. A moderate MET cut is applied MET $>$ 20 GeV due to the rpesence of neutrinos in the final state searched for. Since a High mass signal is searched for, an $m_T^I > 100$ GeV is applied. A cut on the transverse momentum ($p_T^{\ell\ell}$ >30 GeV) and on the $m_T^H > 60$ GeV are applied against $DY \to \tau\tau$ background. Finally, against the top background, all jets above 20 GeV are requested not to be identified as b-jets according to the cMVAv2 tagger, loose WP.

This is the full selection, defined as the "WW OF selection" :

- Two isolated leptons with different charge and flavor ($\mu^{\pm}e^{\mp}$);
- p_T of the leading lepton $>$ 25 GeV;
- p_T of the trailing lepton $>$ 20 GeV;
- Third lepton veto: veto events if a third lepton with $p_T > 10$ GeV;
- $m_{\ell\ell} > 50$ GeV, to reduce H(125) contamination;
- MET $>$ 20 GeV;
- $m_T^I > 100$ GeV;
- $p_T^{\ell\ell}$ >30 GeV;
- $m_T^H > 60$ GeV;
- no b-tagged (cMVAv2 loose WP) jets with $p_T > 20$ GeV;

Events passing the WW OF selection are categorized according to the jet multiplicity, counting jets above 30 GeV, to enhance the sensitivity, especially against the top background.

- **0 jet**, no jets are required in the event;
- **1 jet**, exacly 1 jet is required in the event;
- **2 jet**, exacly 2 jets are required in the event and in addition the condition $\Delta\eta_{jj} < 3.5$ **or** $m_{jj} < 500$ GeV;
- **VBF**, exacly 2 jets are required in the event and in addition the condition $\Delta\eta_{jj} > 3.5$ **and** $m_{jj} > 500$ GeV;

where the 2 jet and VBF regions are mutually exclusive by construction.

To extract high mass boson signals in these four categories, the same strategy as in [1] is followed: the m_T^I distribution is fitted as the sum of signal and background templates. Different binnings have been chosen for the m_T^I distributions in the different categories. The binning was chosen to have at least 10 top MC events in each bin of the template. The chosen bins are:

- **0/1/2 jet**, [100,150,200,250,300,350,400,450,500,550,600,650,700,750,800,900,1000,2000]
- **VBF**, [100,150,200,250,300,350,400,500,700,1000,2000]

where the first number represents the lower edge of the first bin while the other numbers rep- resent the upper edges. The last bin is an overflow bin.

The distributions for the four signal region, still blinded, of m_T^I, m_T^H, $m_{\ell\ell}$ are presented for the four different categories in Figs. 5.2, 5.3, 5.4.

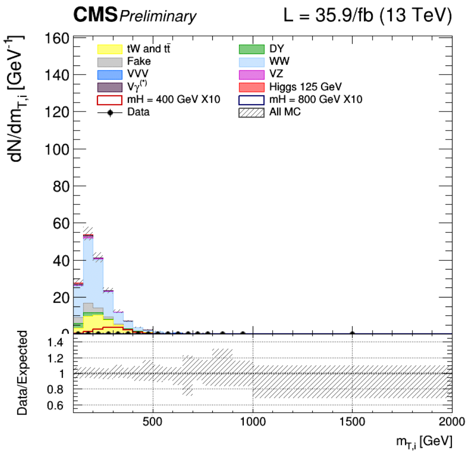

(a) 0 jet

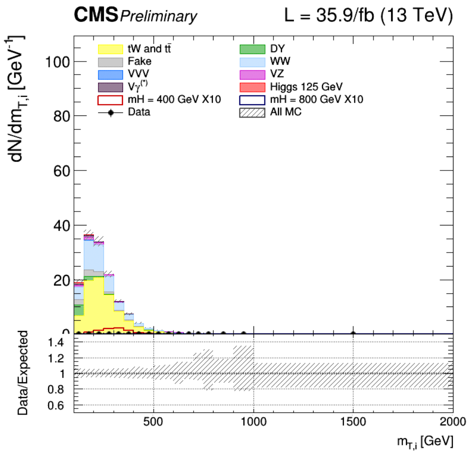

(b) 1 jet

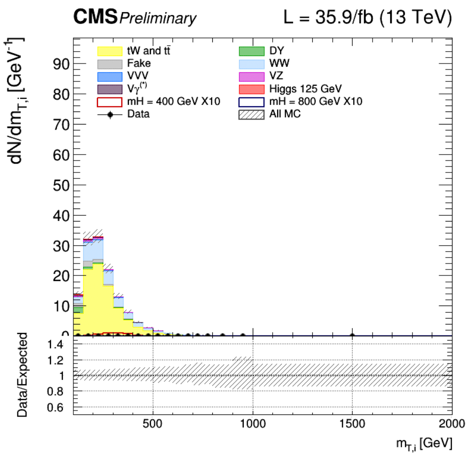

(c) 2 jet

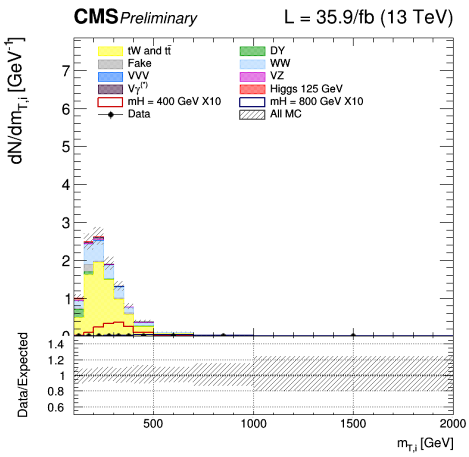

(d) VBF

Figure 5.2. Distributions m_T^I in the signal region for 0, 1, 2 and VBF categories. Two different signal hypothesis corresponding to m_X400 GeV and m_X800 GeV are shown superimposed to the background as a comparison. The binning is different in according to the number of jets.

The different contributin of the signal, the gluon-gluon fusion, the VBS and the interferences are shown separately in Fig. 5.5 for the m_T^I distribution .

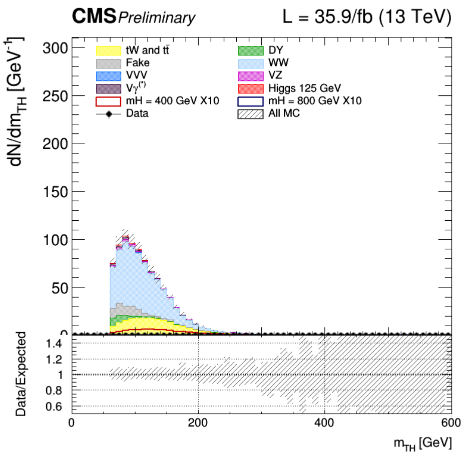

(a) 0 jet

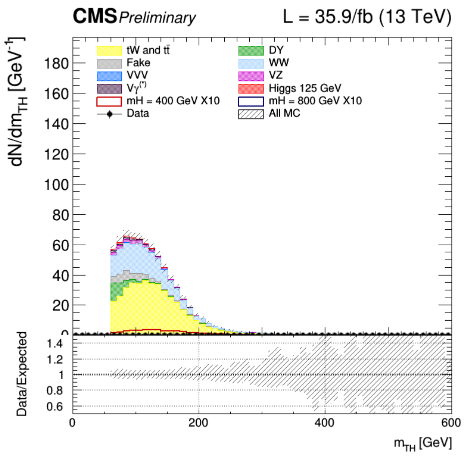

(b) 1 jet

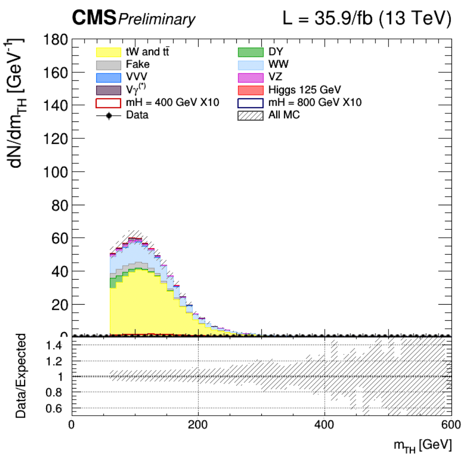

(c) 2 jet

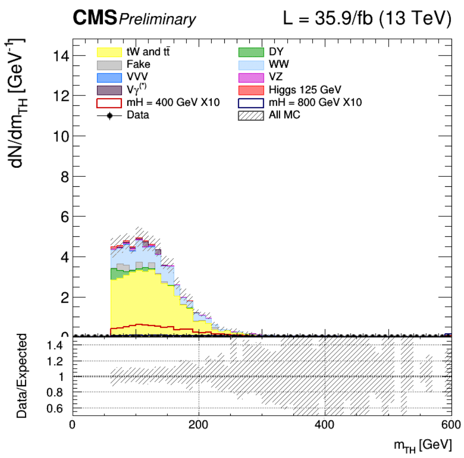

(d) VBF

Figure 5.3. Distributions m_T^H in the signal region for 0, 1, 2 and VBF categories. Two different signal hypothesis corresponding to m_X400 GeV and m_X800 GeV are shown superimposed to the background as a comparison. The binning for m_T^H is the same in the jets categories.

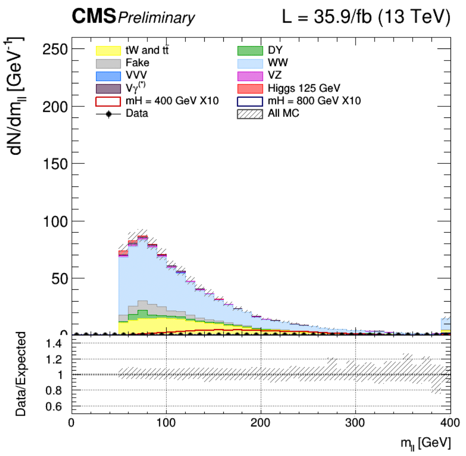

(a) 0 jet

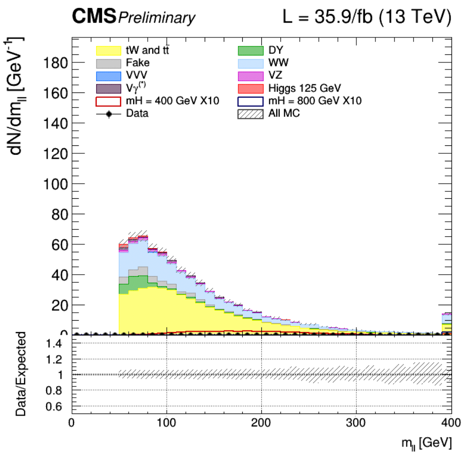

(b) 1 jet

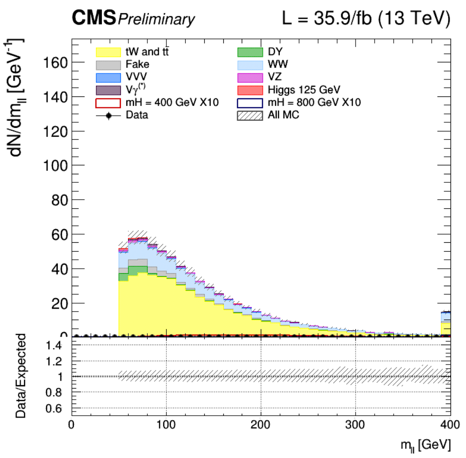

(c) 2 jet

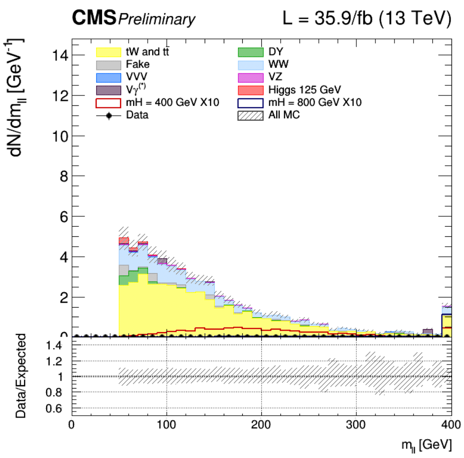

(d) VBF

Figure 5.4. Distributions $m_{\ell\ell}$ in the signal region for 0, 1, 2 and VBF categories. Two different signal hypothesis corresponding to m_X400 GeV and m_X800 GeV are shown superimposed to the background as a comparison. The binning for $m_{\ell\ell}$ is the same in the jets categories.

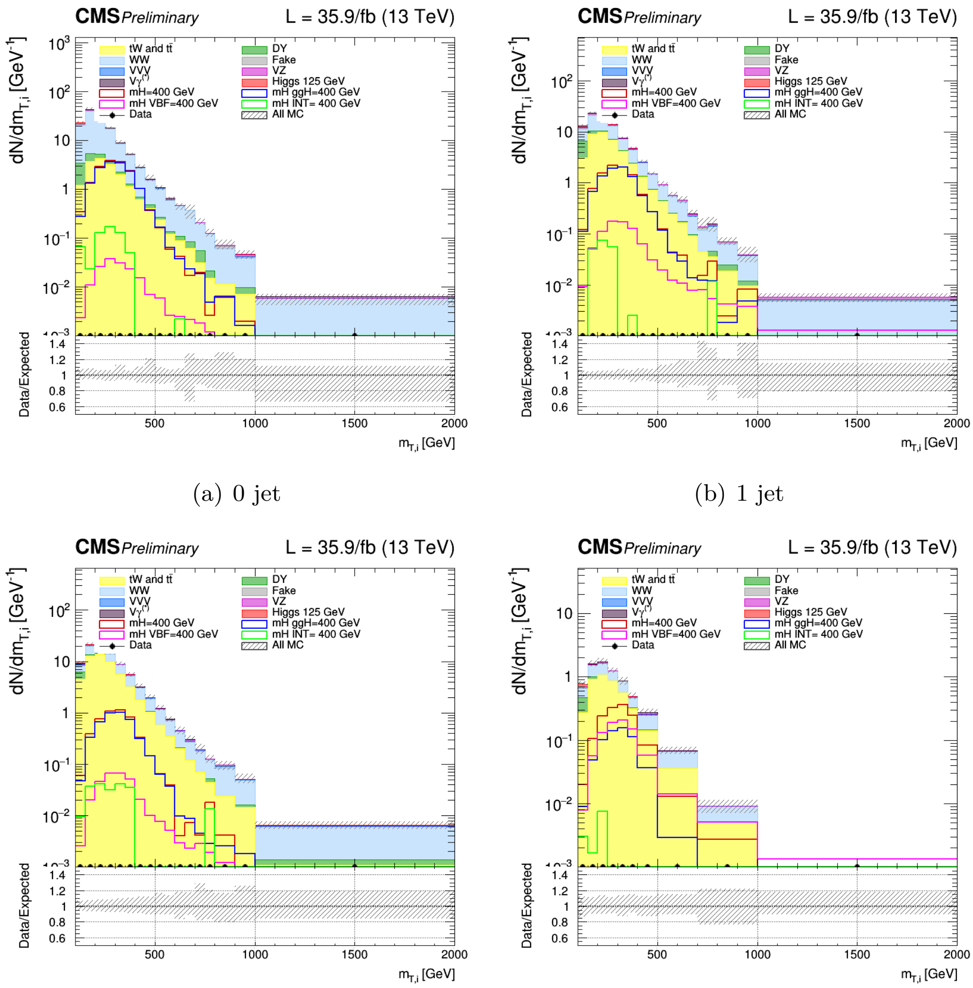

(a) 0 jet

(b) 1 jet

(c) 2 jet

(d) VBF

Figure 5.5. Distributions of the different contribution of the signal for m_T^I in region for 0, 1, 2 and VBF categories. The signal hypothesis corresponding to m_X400. The red line correspond to the Signal (total), the blue line correspond to the gluon-gluon contribution, the violet correspond to the VBF and the green to to total (gluon-gluon+VBF) interference.

5.2.2 Signal region Unblinding

The unblinding m_T^I distribution of the signal regions is shown is Fig. 5.18 and Fig. 5.7

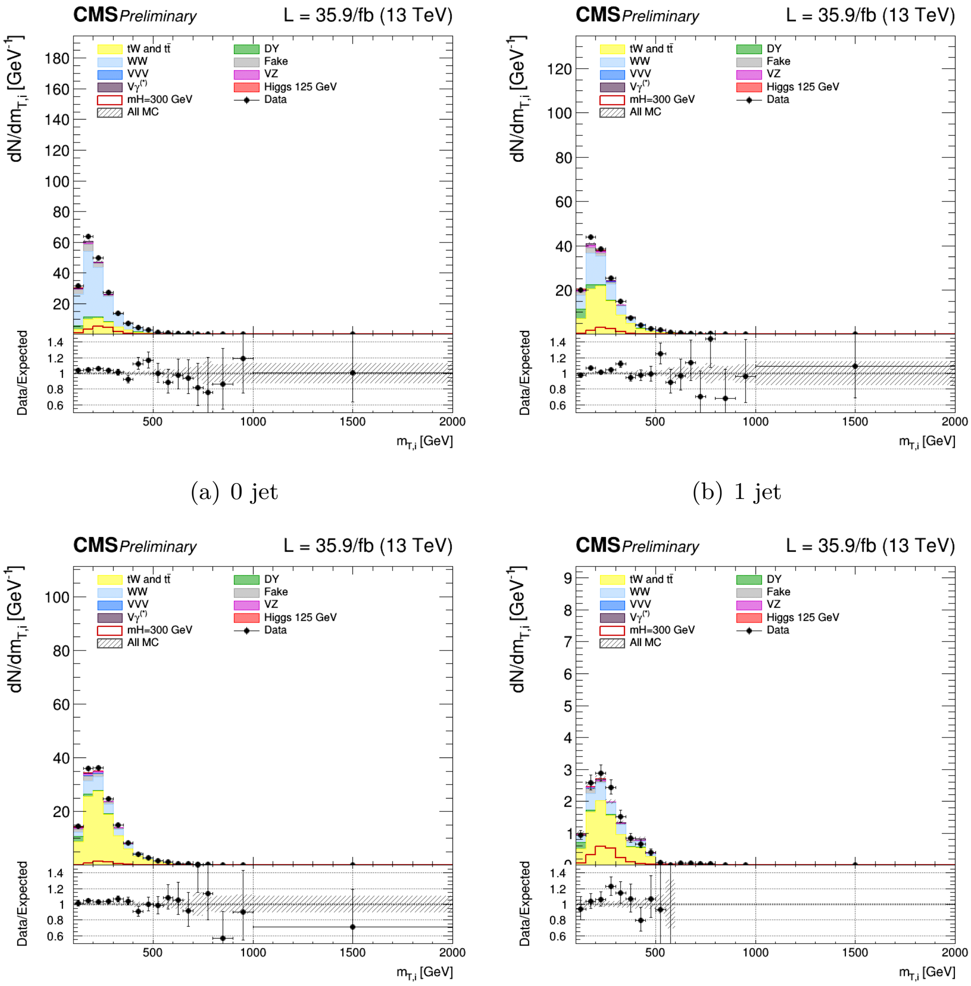

(a) 0 jet (b) 1 jet

(c) 2 jet (d) VBF

Figure 5.6. Unblinding distributions m_T^I in the signal region for 0, 1, 2 and VBF categories. The signal hypothesis corresponding to m_X of 300 GeV.

5.2.3 Background estimation

The main background processes that affect this signature arise from non-resonant WW production and from top production, including tt pairs and single top production (mostly tW), and are estimated using data. Instrumental backgrounds arising from non-prompt leptons in W+jets production and mis-measurement of E_T^{miss} in Drell-Yan events are also estimated from data. The contribution from Wγ^* is estimated partly from data. The contribution of other sub-dominant backgrounds is obtained directly from simulated samples. The different data-driven background

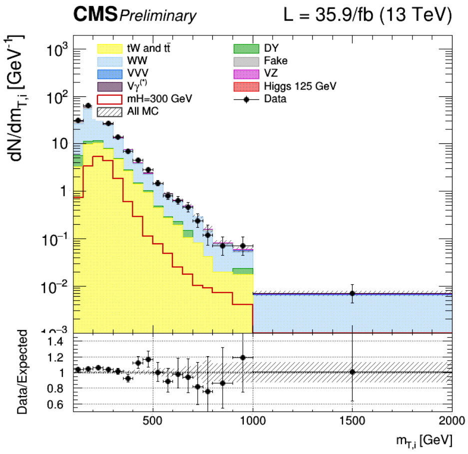

(a) 0 jet

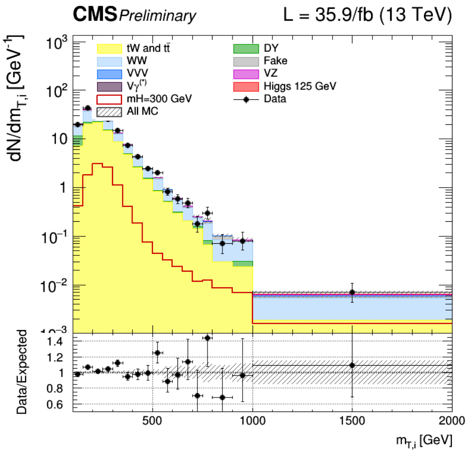

(b) 1 jet

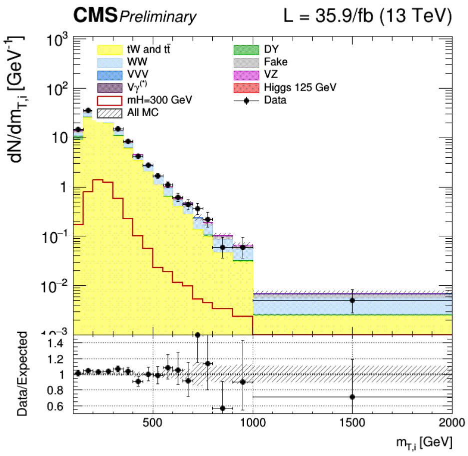

(c) 2 jet

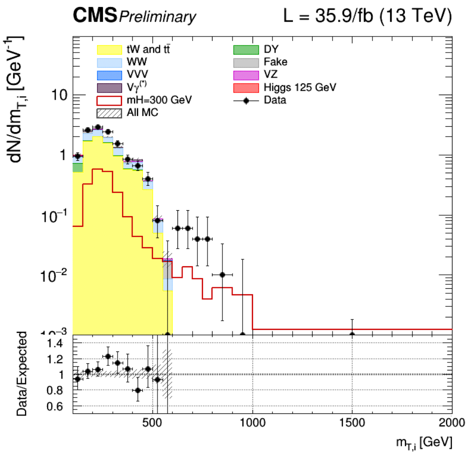

(d) VBF

Figure 5.7. Unblinding distributions m_T^I in the signal region for 0, 1, 2 and VBF categories. The signal hypothesis corresponding to m_X of 300 GeV.

estimations are explained in the following subsections.

More precisely top and DY backgrounds normalizations have been extracted directly from data-simulation comparison in specific control regions enriched in either one or the other background separately for the 0, 1 ,2 and VBF jet categories, using the rateParam feature of the combine package.

5.2.4 Drell-Yan $\tau\tau$ control region

To normalize the Drell-Yan $\tau\tau$ background to the data, control regions have been defined, as close as possible to the signal region, but enriched in Z $\rightarrow \tau^+\tau^-$. In particular, the WW OF selection is used with inverted m_T^H cut, i.e. $m_T^H < 60$. In addition a cut on the invariant mass of the two leptons 50 GeV $< m_{\ell\ell} <$ 80 GeV is requested to exclude possible contribution from non-prompt leptons (low limit) and from tt (high limit).

For each signal category, a corresponding Drell-Yan $\tau\tau$ control regions is defined. We thus have 4 total Drell-Yan $\tau\tau$ control regions, for 0 jets, 1 jets, 2 jets and VBF.

The control plots for several variables in a Drell-Yan enriched phase space for the four jets categories are shown in Figs. 5.8, 5.9, 5.10, 5.11. In general there is a good agreement between data and MC.

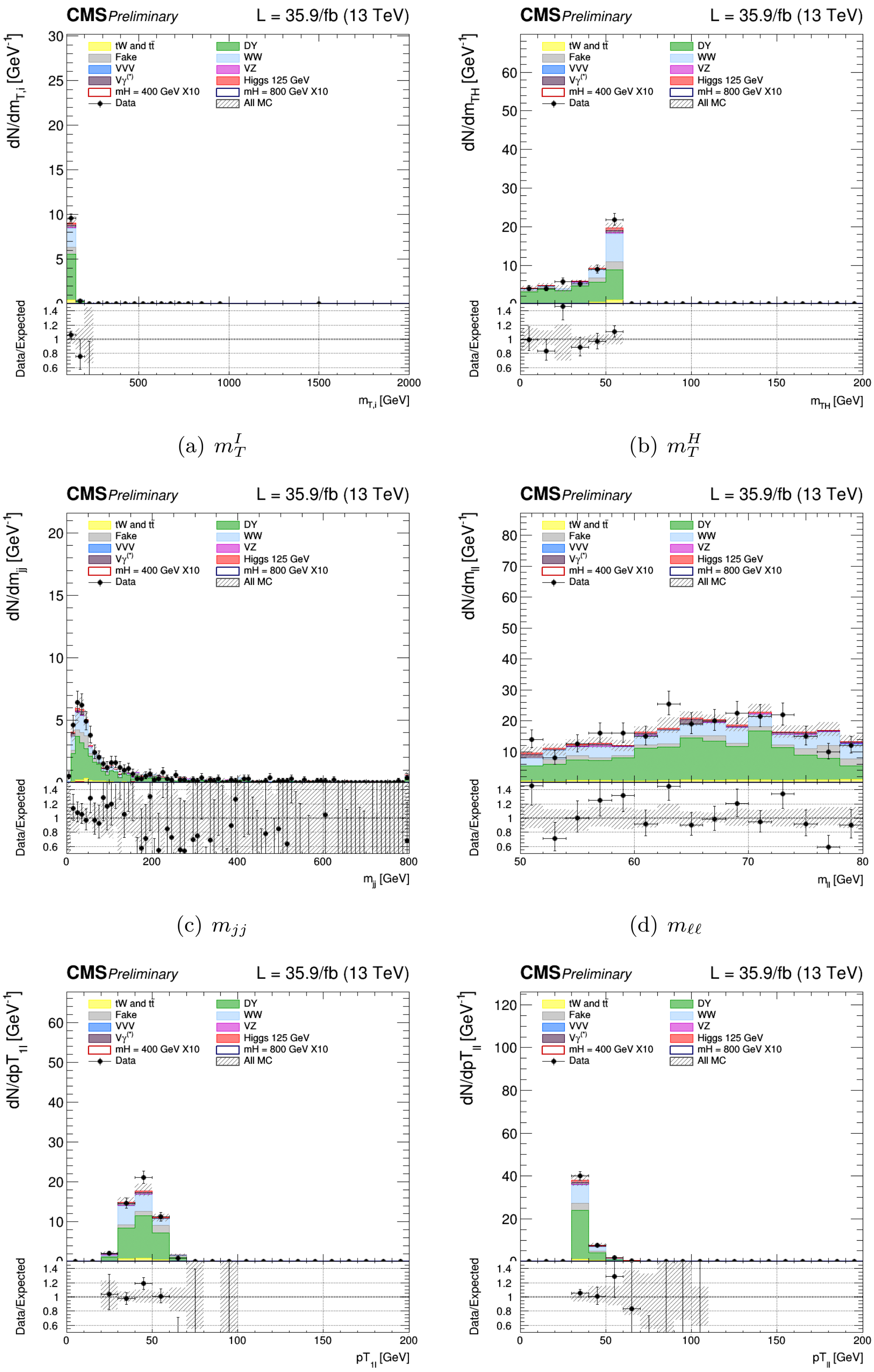

(a) m_T^I

(b) m_T^H

(c) m_{jj}

(d) $m_{\ell\ell}$

(e) p_T leading lepton

(f) $p_T^{\ell\ell}$

Figure 5.8. Control plots for several variables in a Drell-Yan enriched phase space for events with 0 jet.

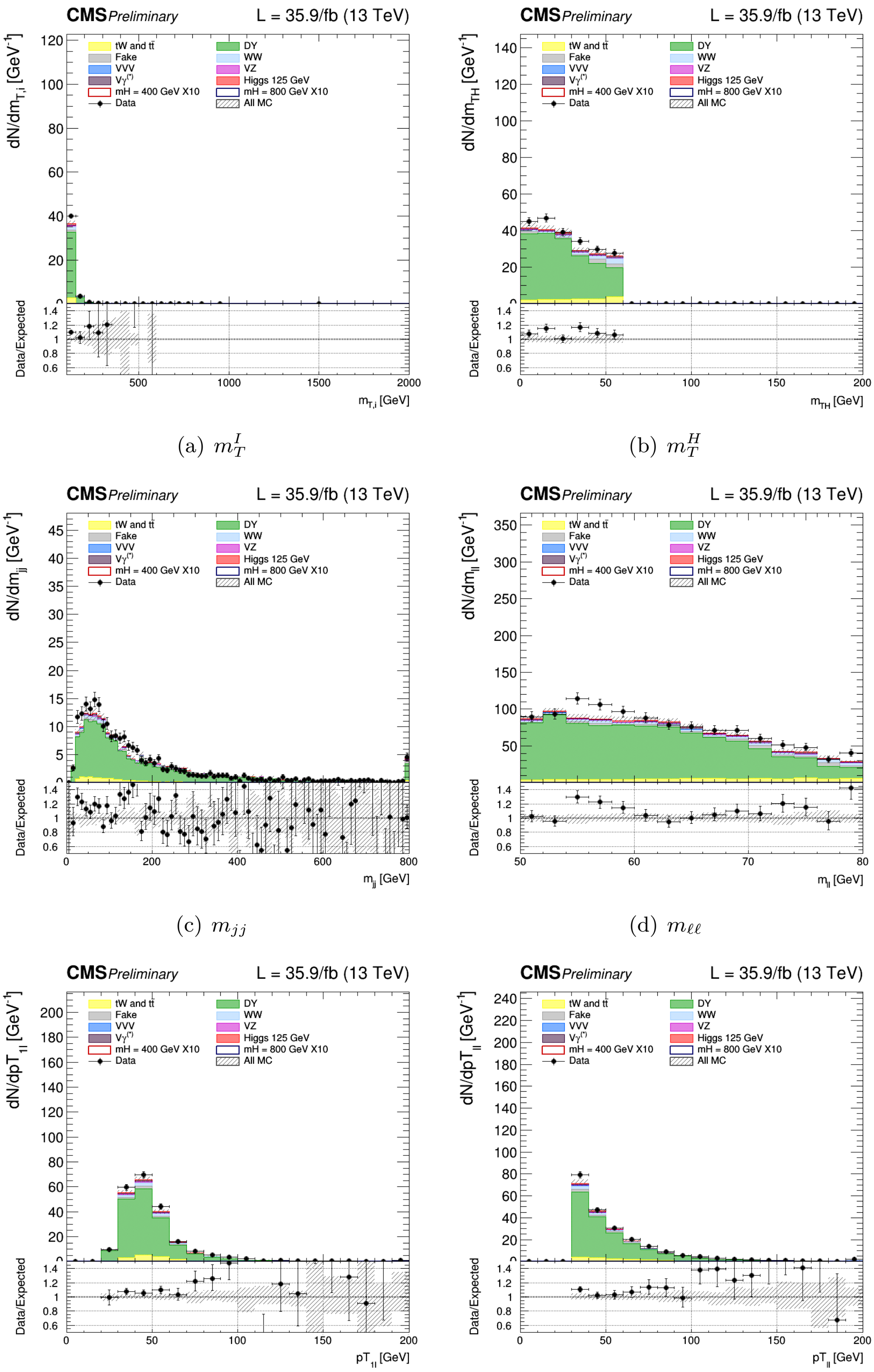

(a) m_T^I

(b) m_T^H

(c) m_{jj}

(d) $m_{\ell\ell}$

(e) p_T leading lepton

(f) $p_T^{\ell\ell}$

Figure 5.9. Control plots for several variables in a Drell-Yan enriched phase space for events with 1 jet.

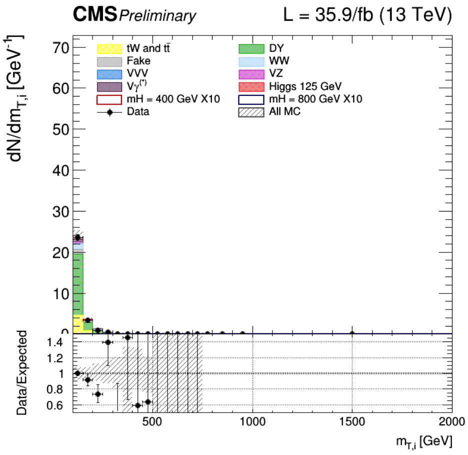

(a) m_T^I

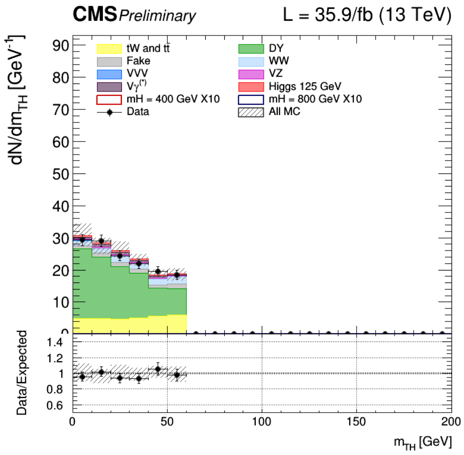

(b) m_T^H

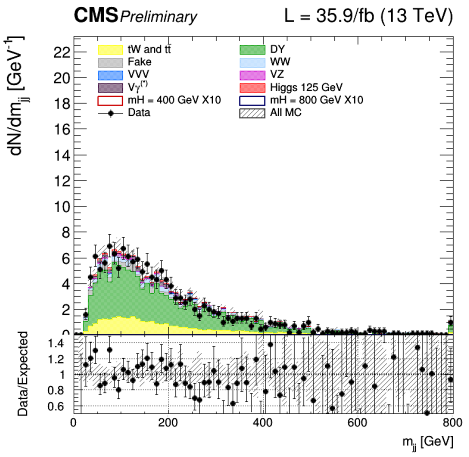

(c) m_{jj}

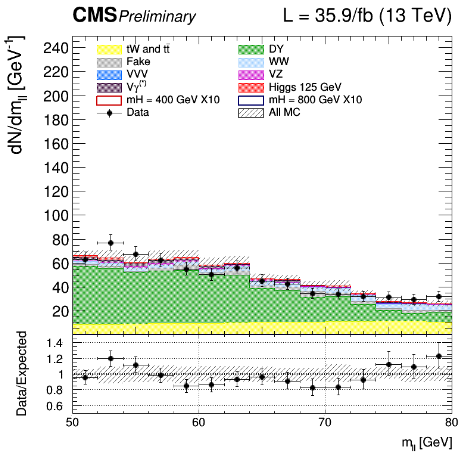

(d) $m_{\ell\ell}$

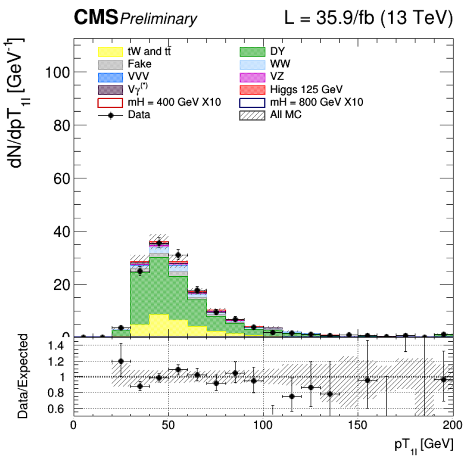

(e) p_T leading lepton

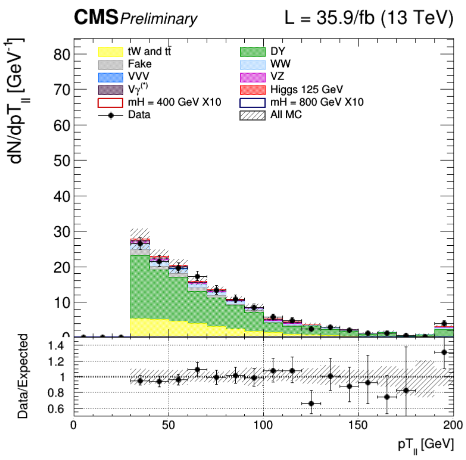

(f) $p_T^{\ell\ell}$

Figure 5.10. Control plots for several variables in a Drell-Yan enriched phase space for events with 2 jet.

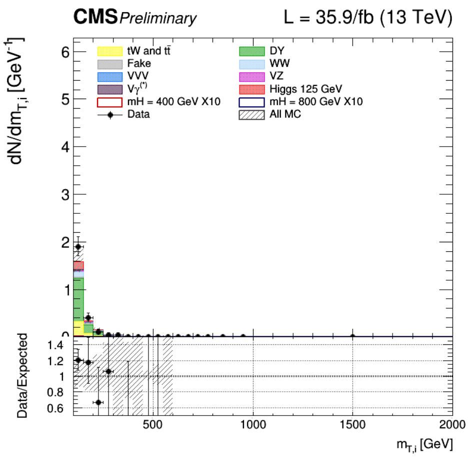

(a) m_T^I

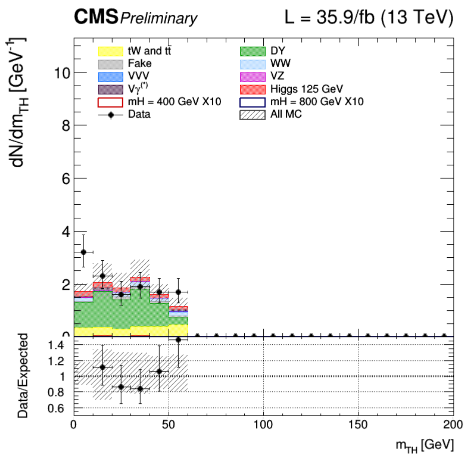

(b) m_T^H

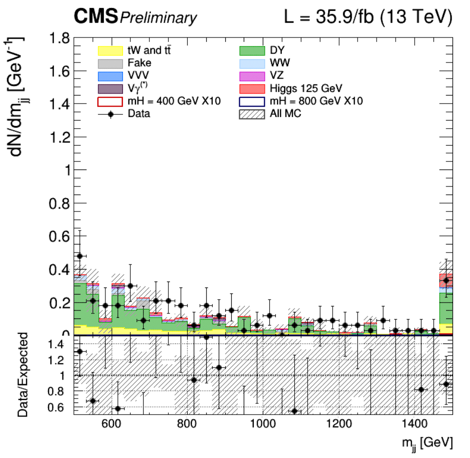

(c) m_{jj}

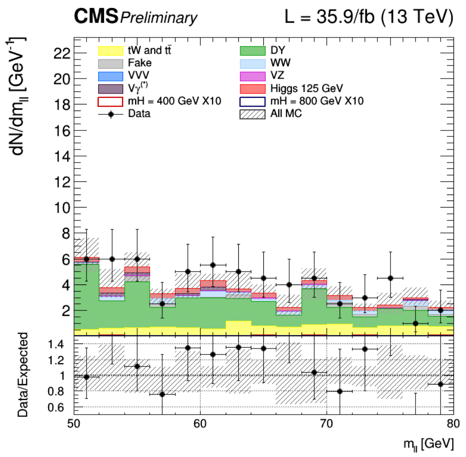

(d) $m_{\ell\ell}$

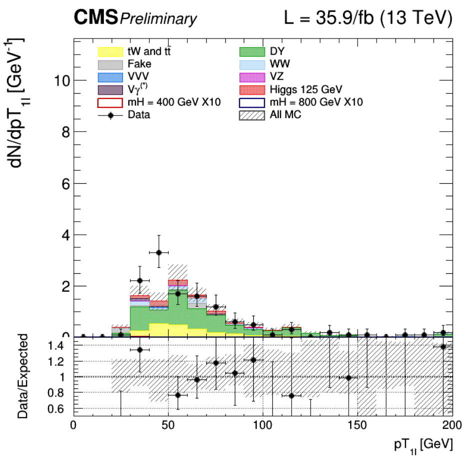

(e) p_T leading lepton

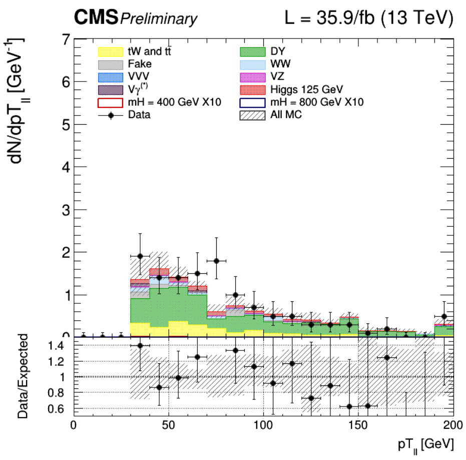

(f) $p_T^{\ell\ell}$

Figure 5.11. Control plots for several variables in a Drell-Yan enriched phase space for events for VBF.

5.2.5 Top control region

Similarly to the DY $\tau\tau$ case, control regions are defined for the top background, and are used to normalize the top background to data. The WW OF selection is used with inversion of the veto on b-jets. In particular the following conditions are imposed to select a top enriched control region for each of the 4 signal regions:

- **0 jet**, at least one b-tagged jet with $20 < p_T < 30$ GeV is required;
- **1 jet**, exactly one b-tagged jet with p_T above 30 GeV is required;
- **2 jet**, exacly 2 jets with at least one of them b-tagged and in addition the condition $\Delta\eta_{jj} < 3.5$ **or** $m_{jj} < 500$ GeV;
- **VBF**, exacly 2 jets with at least one of them b-tagged and in addition the condition $\Delta\eta_{jj} > 3.5$ **and** $m_{jj} > 500$ GeV.

A jet is considered b-tagged if its cMVAv2 score is above the threshold defining the loose working point.

The control plots for several variables in a top enriched phase space for events are shown in the Fig. below. The last bin in the distribution is the overflow.

5.3 Same Flavor final state

The analysis if the same-flavour final state $W^+W^- \to \mu^\pm\mu^\mp 2\nu$ and $W^+W^- \to e^\pm e^\mp 2\nu$ is described in this section.

5.3.1 Signal region

Events are requested to pass single or double lepton triggers and all the physics objects definitions are the same as in the OF analysis. The final state consists of two well identified electrons or two muons with $p_T > 20$ GeV, opposite charge, and large missing transverse energy from the undetected neutrinos.
In addition to the backgrounds described for the OF final state, the background from DY $\to \mu^+\mu^-$ and DY $\to e^+e^-$ is very large in this final state. Indeed, due to this very large background, the SF analysis only targets the VBF topology, where the DY background is suppressed by the tight jet requirements. In addition, an invariant mass of the two leptons larger than 120 GeV is requested. The full selection, defined as the "WW SF selection", is :

- Two isolated leptons with same flavor and opposite charge ($\mu^\pm\mu^\mp$ and $e^\pm e^\mp$);
- p_T of the leading and trailing lepton > 20 GeV;
- Third lepton veto: veto events if a third lepton with $p_T > 10$ GeV;
- $m_{\ell\ell} > 120$ GeV
- $p_T^{\ell\ell}$ >30 GeV;

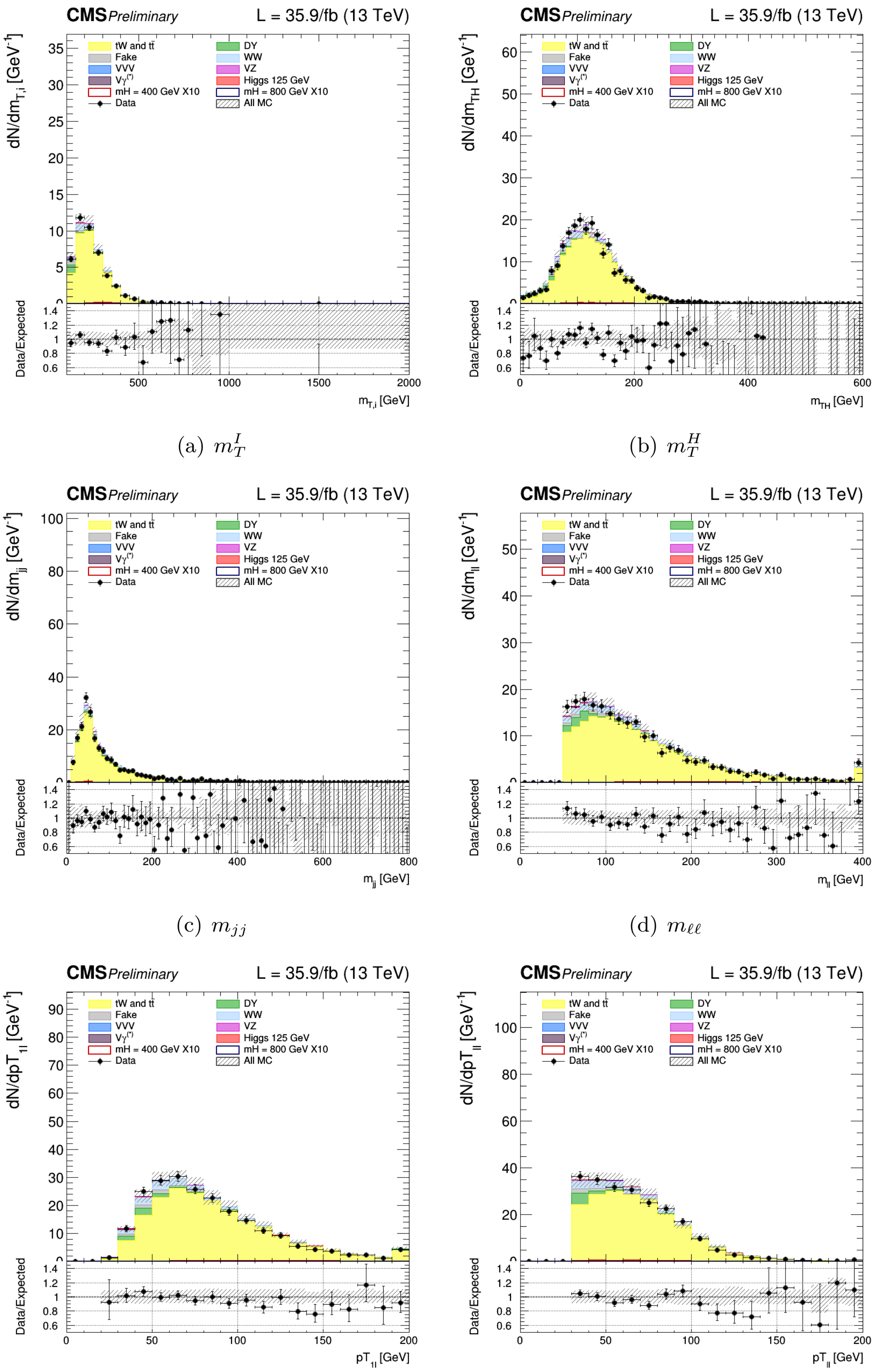

(a) m_T^I

(b) m_T^H

(c) m_{jj}

(d) $m_{\ell\ell}$

(e) p_T leading lepton

(f) $p_T^{\ell\ell}$

Figure 5.12. Control plots for several variables in the Top enriched phase space for events with 0 jet.

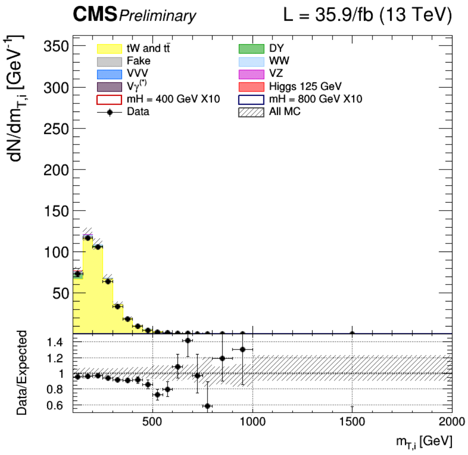

(a) m_T^I

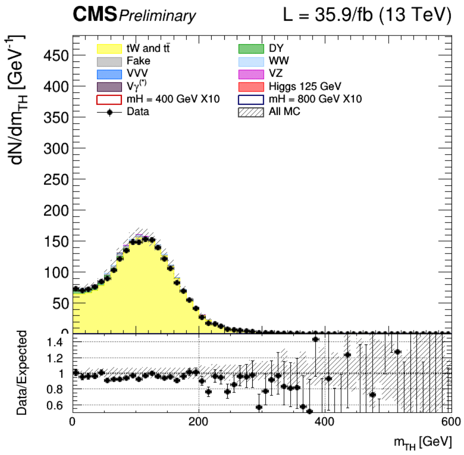

(b) m_T^H

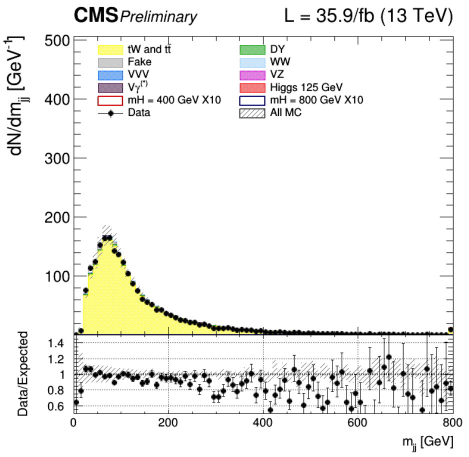

(c) m_{jj}

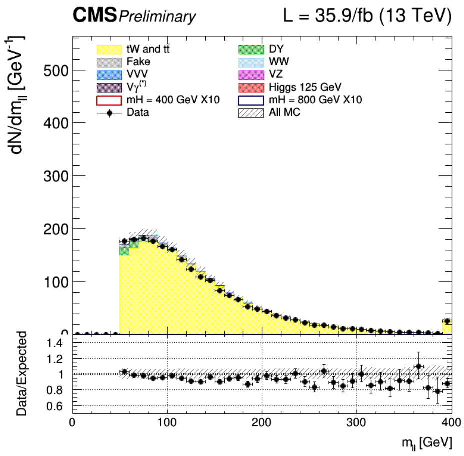

(d) $m_{\ell\ell}$

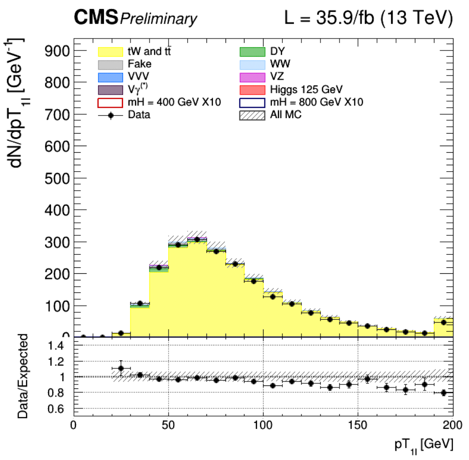

(e) p_T leading lepton

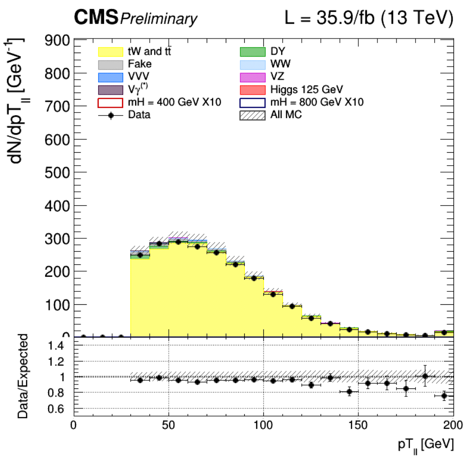

(f) $p_T^{\ell\ell}$

Figure 5.13. Control plots for several variables in the Top enriched phase space for events with 1 jet.

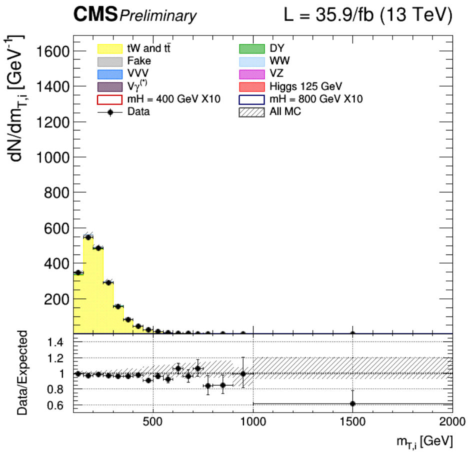

(a) m_T^I

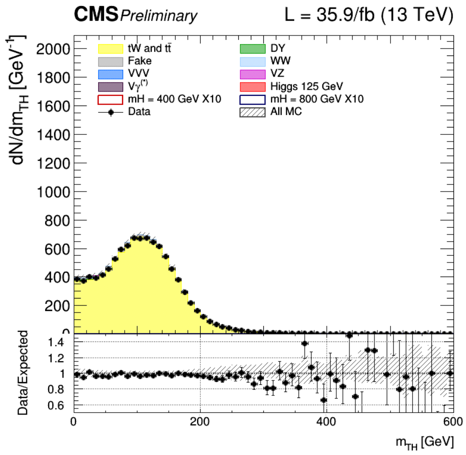

(b) m_T^H

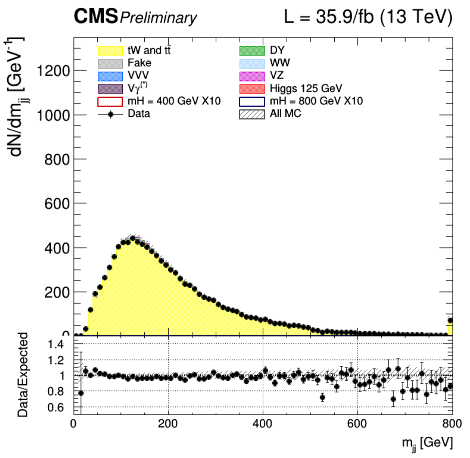

(c) m_{jj}

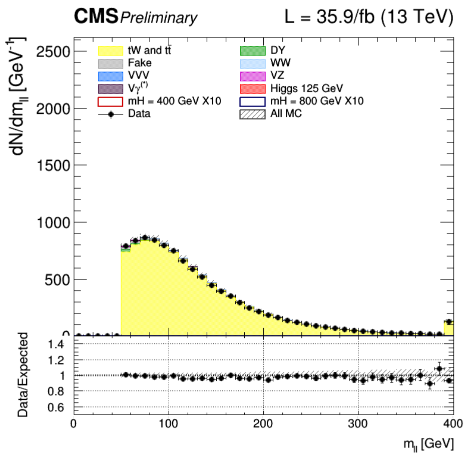

(d) $m_{\ell\ell}$

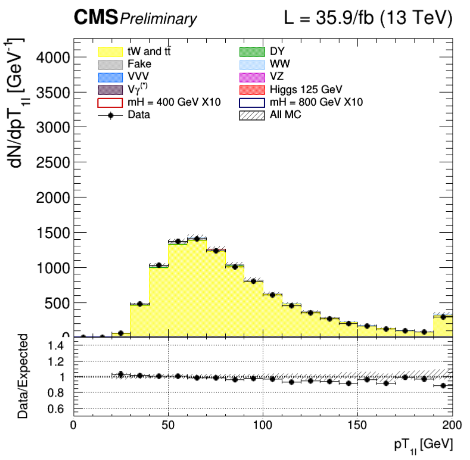

(e) p_T leading lepton

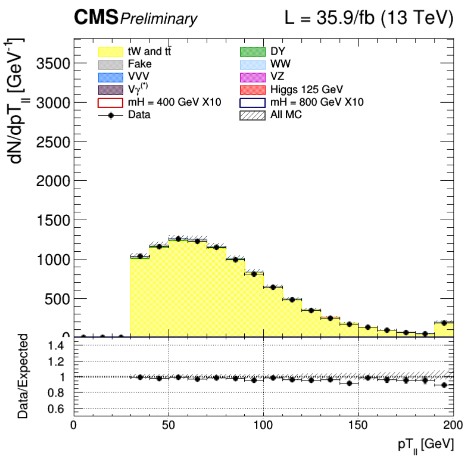

(f) $p_T^{\ell\ell}$

Figure 5.14. Control plots for several variables in the Top enriched phase space for events with 2 jet.

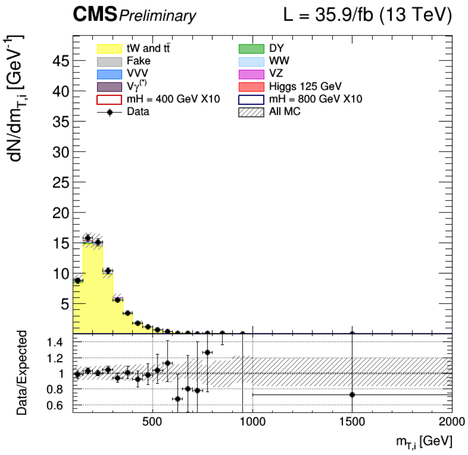

(a) m_T^I

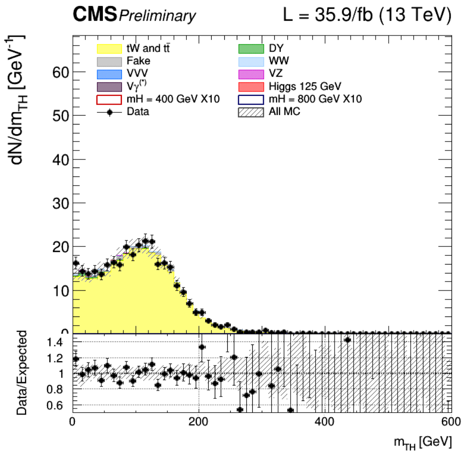

(b) m_T^H

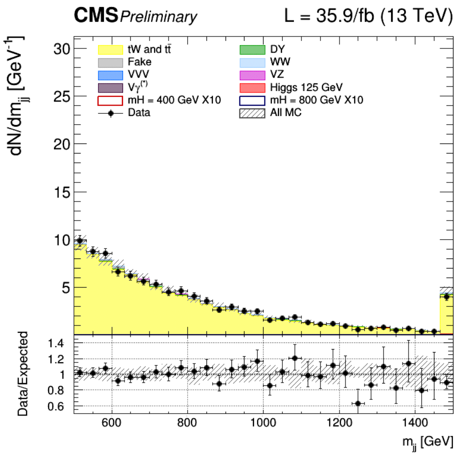

(c) m_{jj}

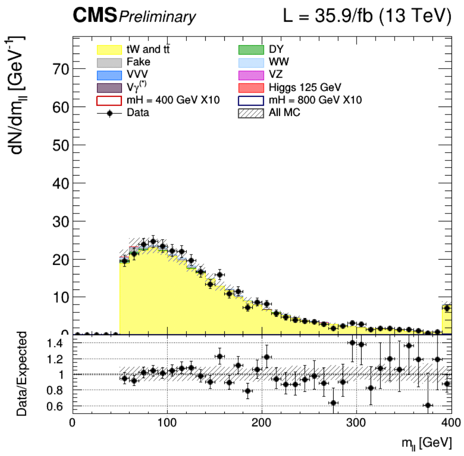

(d) $m_{\ell\ell}$

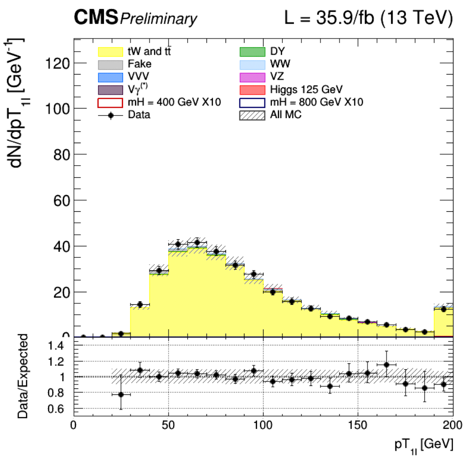

(e) p_T leading lepton

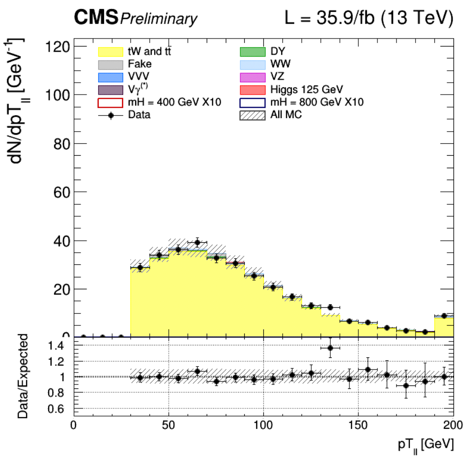

(f) $p_T^{\ell\ell}$

Figure 5.15. Control plots for several variables in the Top enriched phase space for events in VBF region.

- MET > 50 GeV;
- $m_T^I > 100$ GeV;
- At lest 2 jets non b-tagged (according to cMVAv2 loose WP) with $p_T > 30$ GeV.
- $\Delta\eta_{jj} > 3.5$;
- $m_{jj} > 500$ GeV;;

Similarly to the OF analysis, the signal is extracted from a template fit of the m_T^I distribution. The m_T^I distributions has the following binning:

- **VBF**, [100,150,200,250,300,350,400,450,500,600,700,1000];

where the first number represents the lower edge of the first bin while the other numbers represent the upper edges. The last bin is an overflow bin. The binning has been chosen in order to have at least 10 expected Top-backgrounds event and at least 10 expected Drell-Yan events in each bin of the template.
The distributions for the signal region, still blinded, of m_T^I, m_T^H, $m_{\ell\ell}$ and m_{jj} are presented for the $\mu^\pm\mu^\mp$ and $e^\pm e^\mp$ case in Figs. 5.16 and 5.17.

5.3.2 Signal region Unblinding

The unblinding m_T^I distribution of the signal regions is shown is Fig. 5.18 and Fig. 5.7

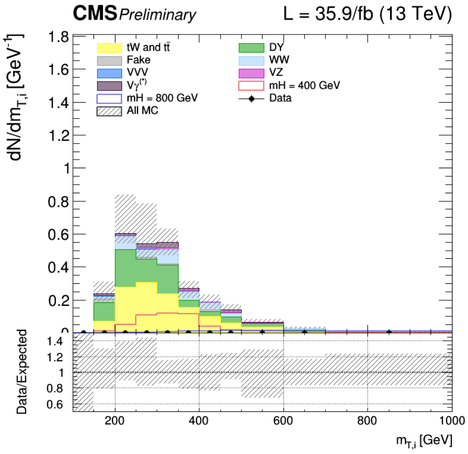

(a) m_T^I

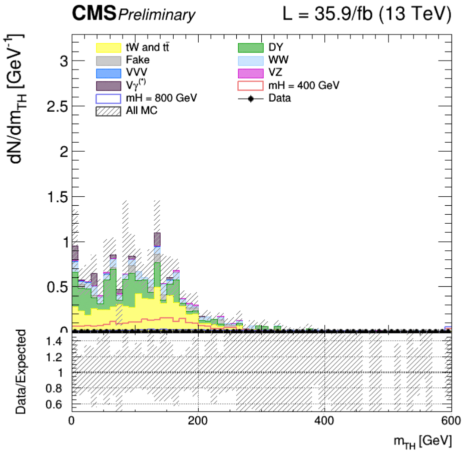

(b) m_T^H

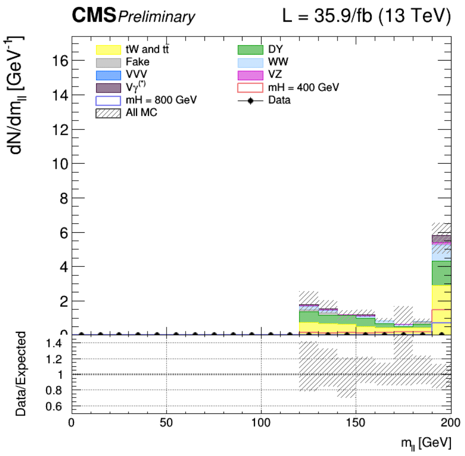

(c) $m_{\ell\ell}$

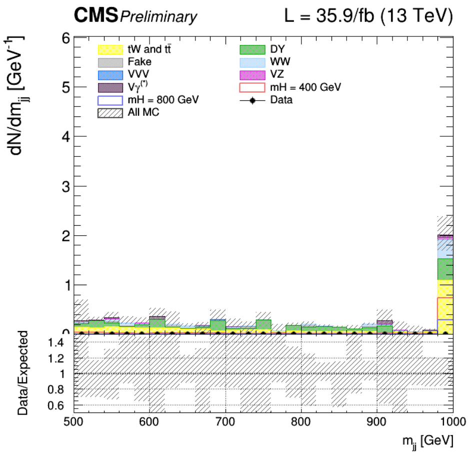

(d) m_{jj}

Figure 5.16. Distributions m_T^I, m_T^I, m_T^H, $m_{\ell\ell}$ and m_{jj} in the signal region $e^{\pm}e^{\mp}$ case. Two different signal hypothesis corresponding to m_X =400 GeV and m_X =800 GeV are shown superimposed to the background as a comparison.

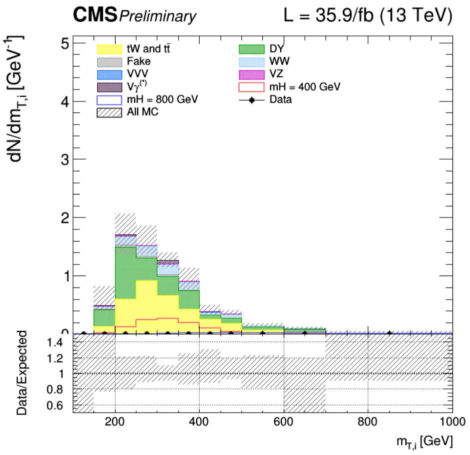

(a) m_T^I

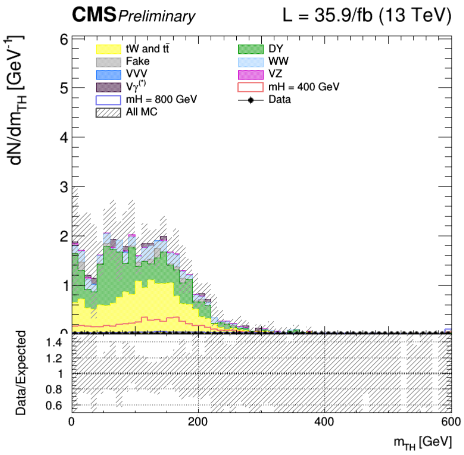

(b) m_T^H

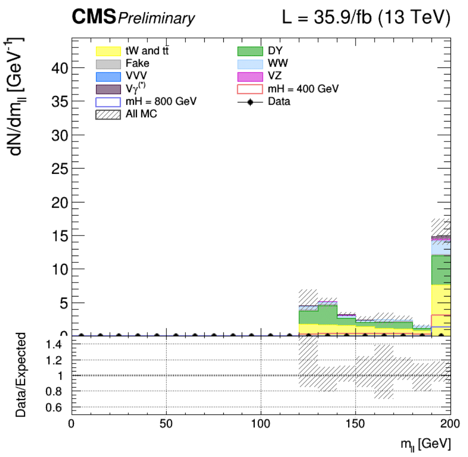

(c) $m_{\ell\ell}$

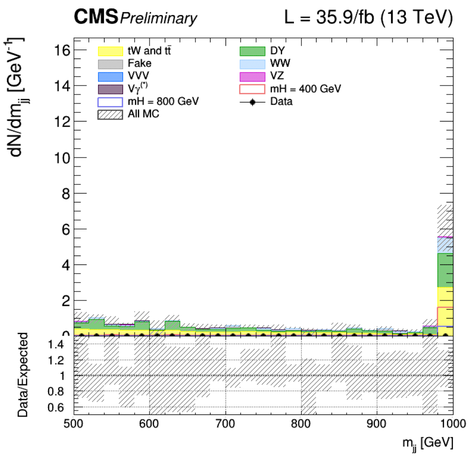

(d) m_{jj}

Figure 5.17. Distributions m_T^I, m_T^I, m_T^H, $m_{\ell\ell}$ and m_{jj} in the signal region $\mu^\pm\mu^\mp$ case. Two different signal hypothesis corresponding to m_X =400 GeV and m_X =800 GeV are shown superimposed to the background as a comparison.

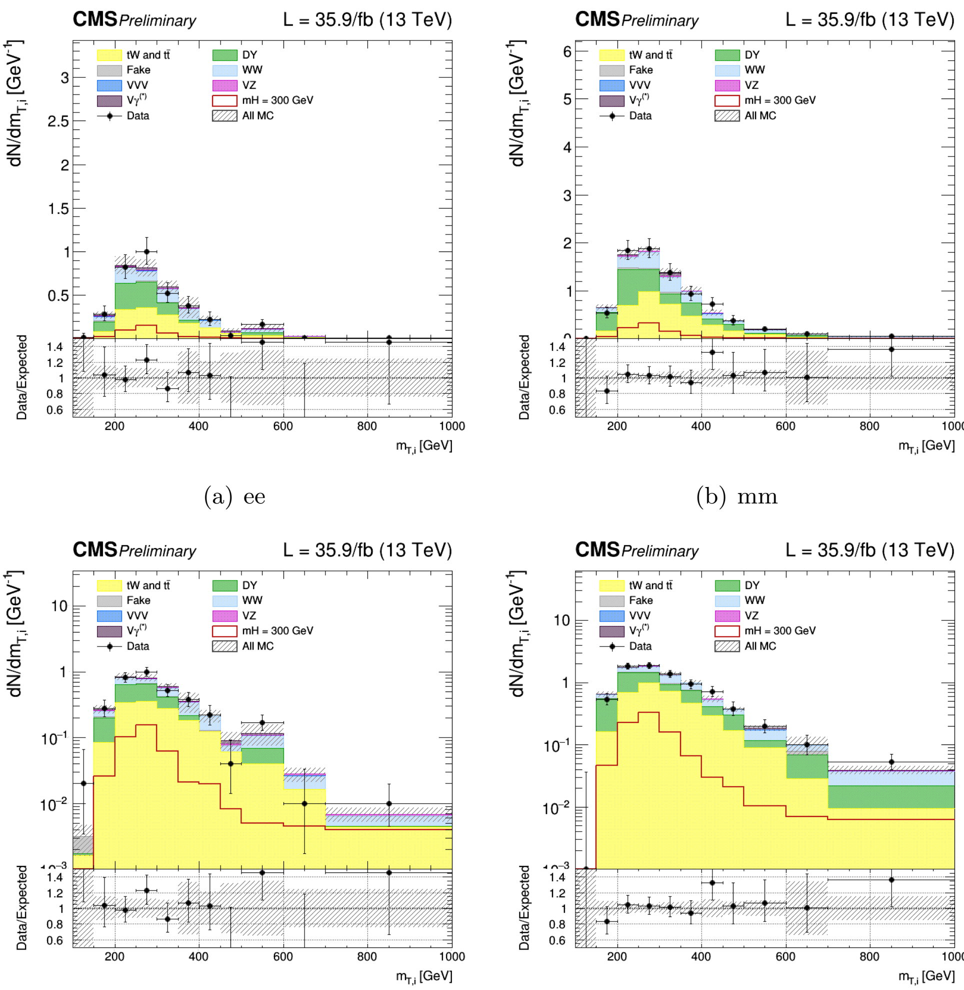

(a) ee

(b) mm

(c) ee

(d) mm

Figure 5.18. Unblinding distributions m_T^I in the signal region for ee and $\mu\mu$ categories in linear and log scale. The signal hypothesis corresponding to m_X of 300 GeV.

5.3.3 Drell-Yan control region

The main background for the SF analysis is the DY. A control region has been defined, as close as possible to the signal one to be used for the normalization of the DY background, separately for electrons an muons.
The control region is defined by the "WW SF selection", except for the $m_{\ell\ell}$ requirement which is changed to 70 GeV $< m_{\ell\ell} <$ 120 GeV to include the Z boson.

The Missing Transverse Energy ditribution in the data shows discrepancies respect to Monte Carlo simulation in ee and $\mu\mu$ Drell-Yan control regions. A correction is applied reweighting all the simulated samples with a weight per event which depends on the MET value. The weight is evaluated as the ratio between data, one subtracted all backgraounds except the DY, and the Drell-Yan itself, in each bins of the distribution, separately for ee and $\mu\mu$ categories. The weight is assumed to be linear as function of the MET value.
This kind of reweighting allows to correct for shape differences between data and MC, , Fig. 5.19.

The control plots for several variables in a Drell-Yan enriched phase space for the ee and $\mu\mu$ are shown in Figs. 5.21 for the dielectron case and Figs. 5.22 for the dimuon case. In general there is a good agreement betwen data and MC.

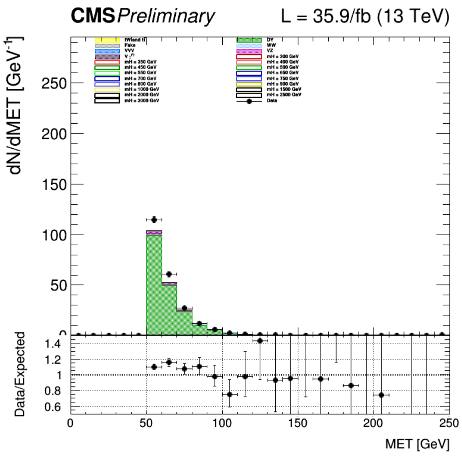

(a) ee before the reweight

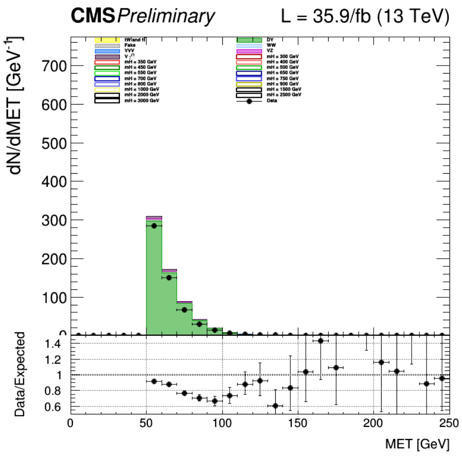

(b) $\mu\mu$ before the reweight

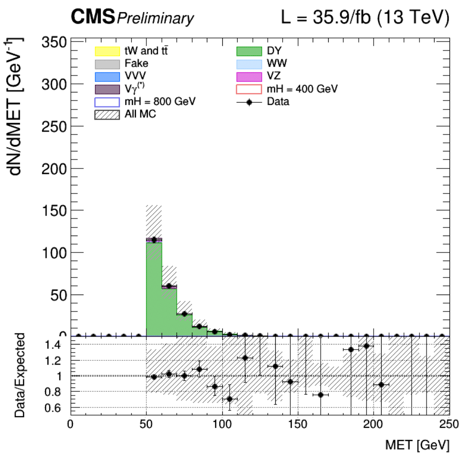

(c) ee after the reweight

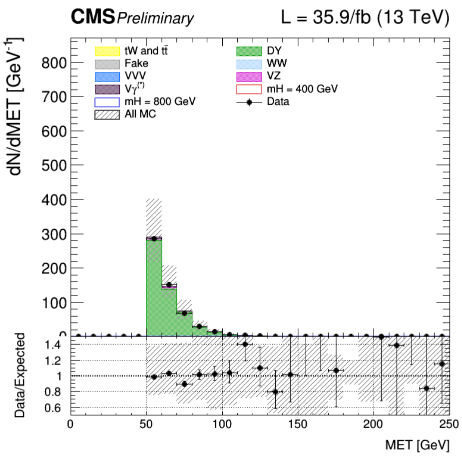

(d) $\mu\mu$ after the reweight

Figure 5.19. MET control plots for Drell-Yan fot ee categories in a and for $\mu\mu$ in b before the reweight. In c and d the same distribution after the correction.

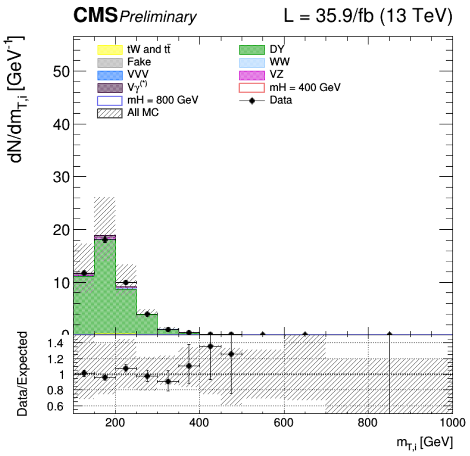

(a) m_T^I

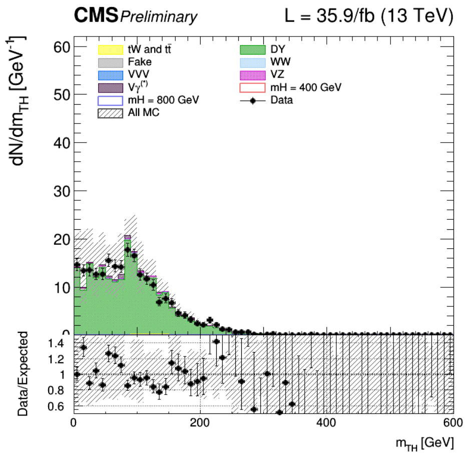

(b) m_T^H

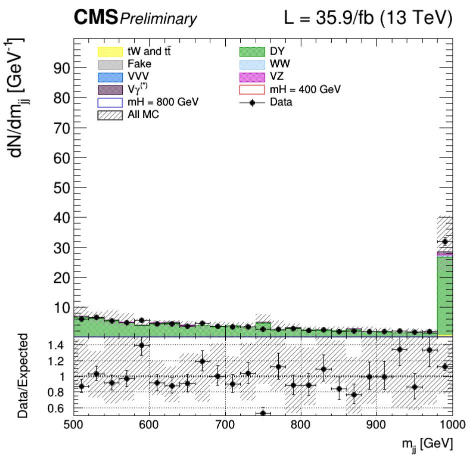

(c) m_{jj}

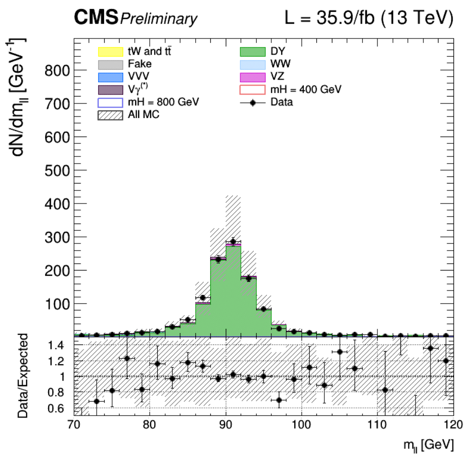

(d) $m_{\ell\ell}$

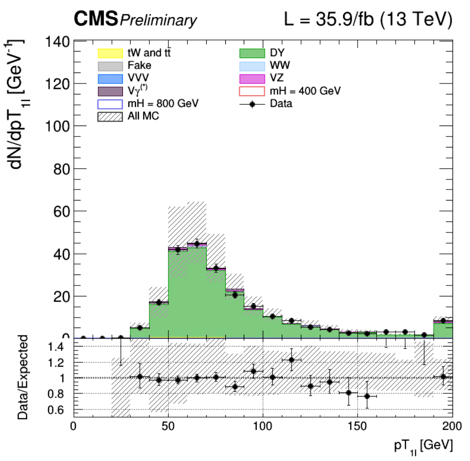

(e) p_T leading lepton

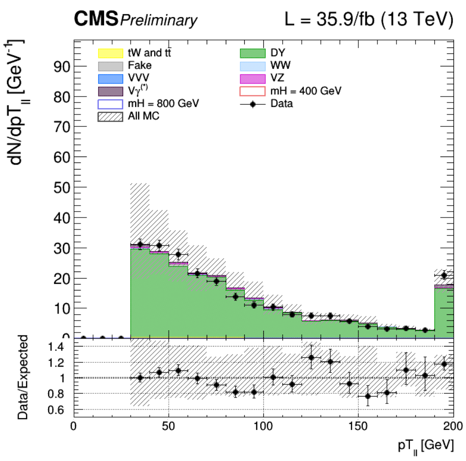

(f) $p_T^{\ell\ell}$

Figure 5.20. Control plots for several variables in a Drell-Yan enriched phase space for ee.

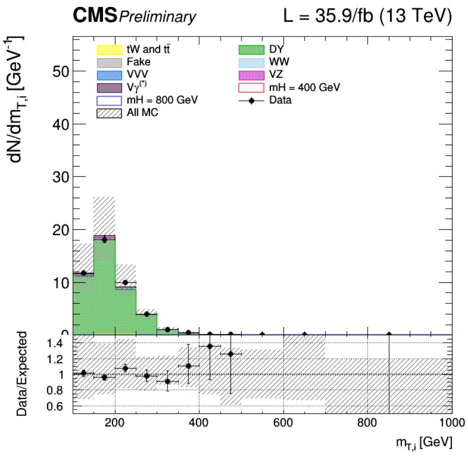

(a) m_T^I

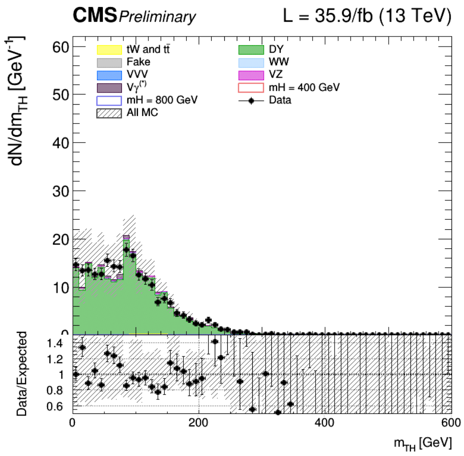

(b) m_T^H

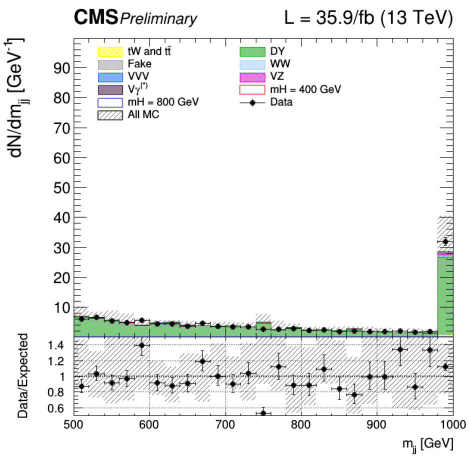

(c) m_{jj}

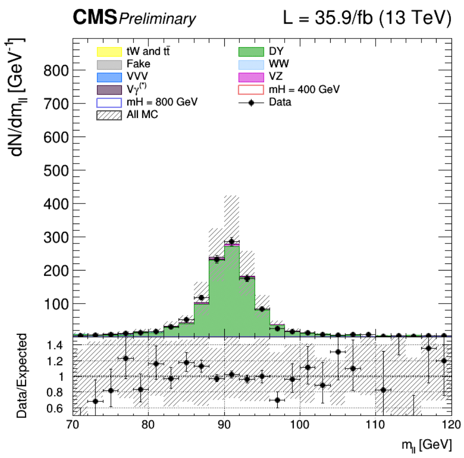

(d) $m_{\ell\ell}$

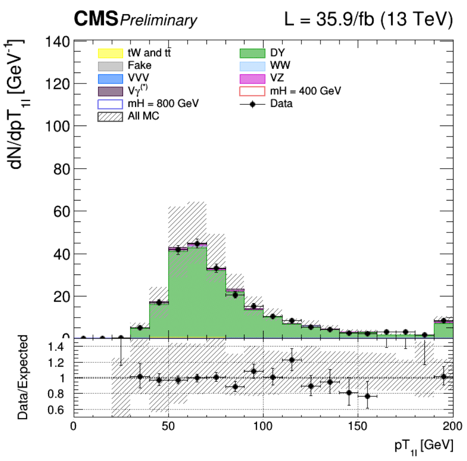

(e) p_T leading lepton

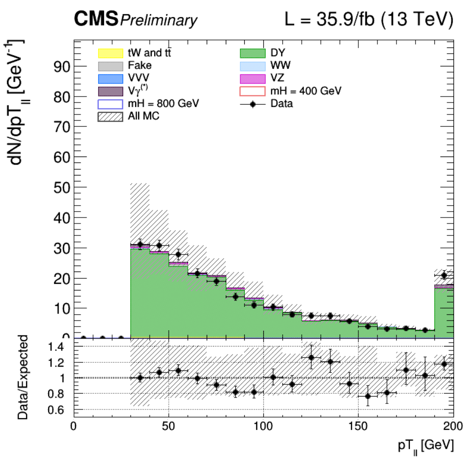

(f) $p_T^{\ell\ell}$

Figure 5.21. Control plots for several variables in a Drell-Yan enriched phase space for ee.

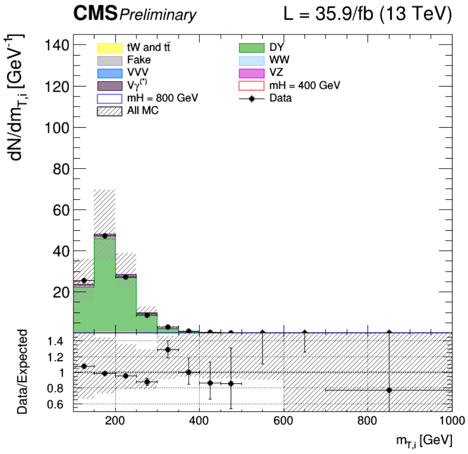

(a) m_T^I

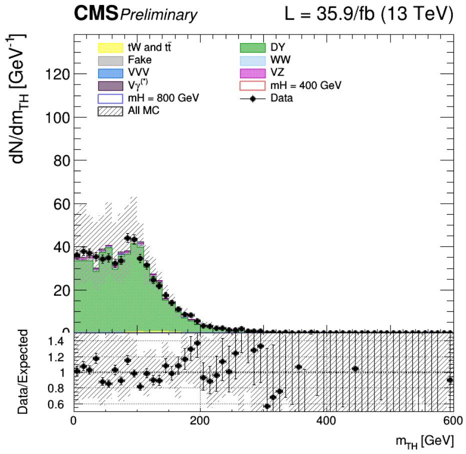

(b) m_T^H

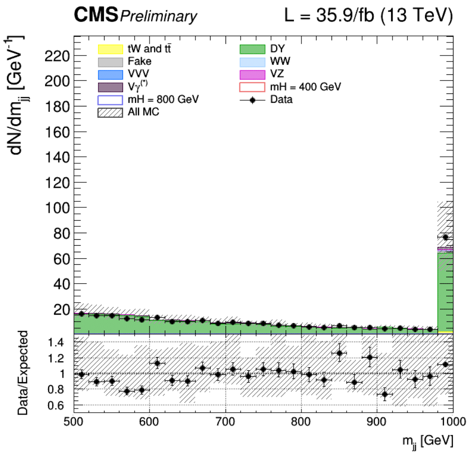

(c) m_{jj}

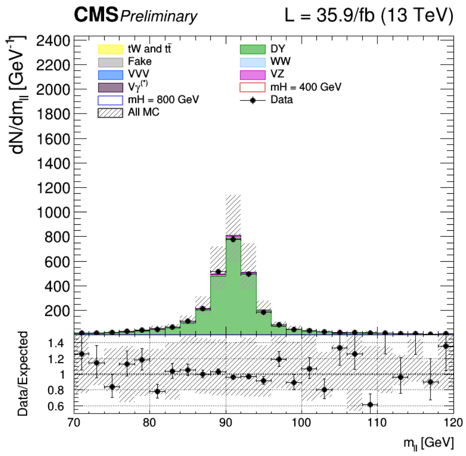

(d) $m_{\ell\ell}$

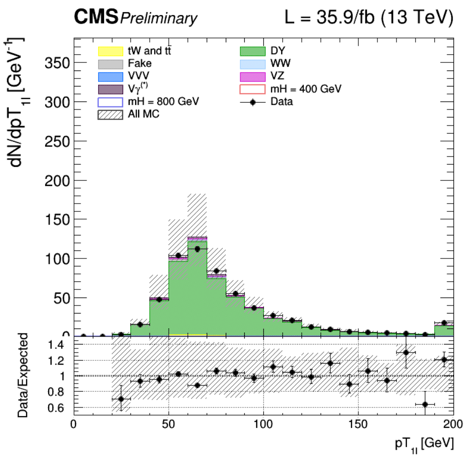

(e) p_T leading lepton

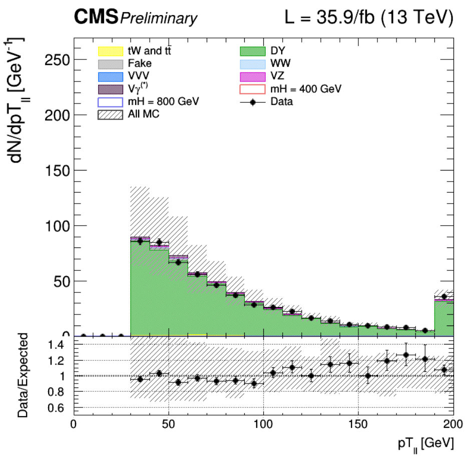

(f) $p_T^{\ell\ell}$

Figure 5.22. Control plots for several variables in a Drell-Yan enriched phase space for $\mu\mu$.

5.3.4 Top control region

A top-enriched control region is defined to normalize the top backgrouns, separately for electrons and muons. The "WW SF selection" is required with the inversion of the b-tagging requirement, i.e. the two jets are both requested to be b-tagged according to cMVAv2 loose WP.:

The control plots for several variables in a top enriched phase space for events are shown in the Figs. 5.23 for the dielectron case and 5.24 for the dimuon case. Good agreement is observed between data and MC.

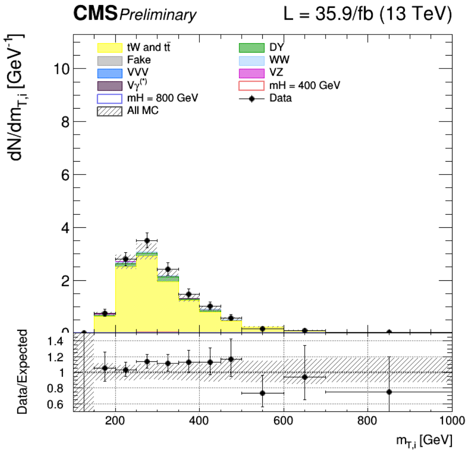

(a) m_T^I

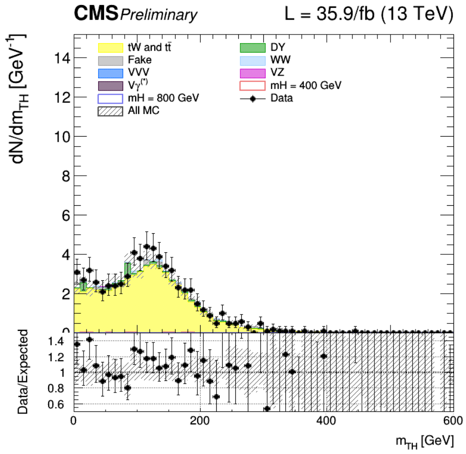

(b) m_T^H

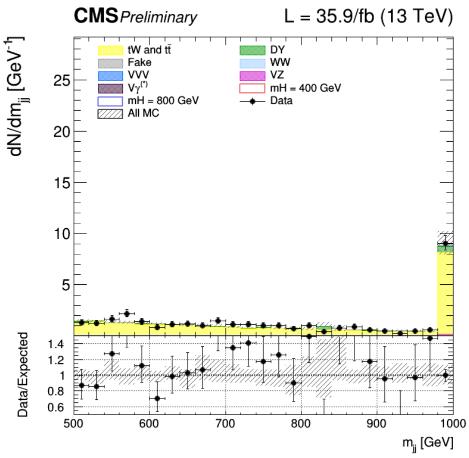

(c) m_{jj}

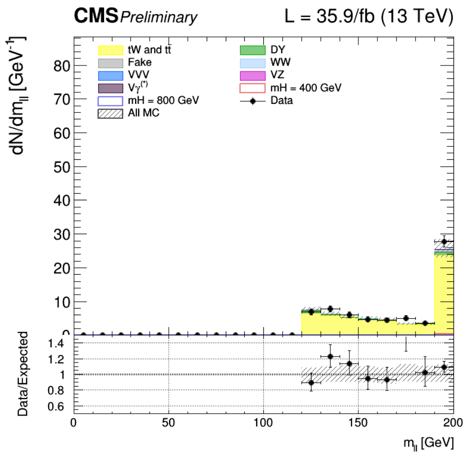

(d) $m_{\ell\ell}$

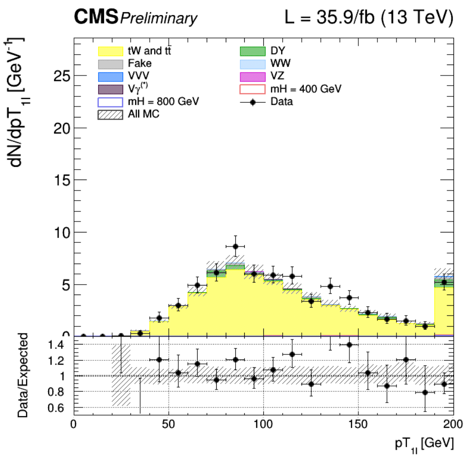

(e) p_T leading lepton

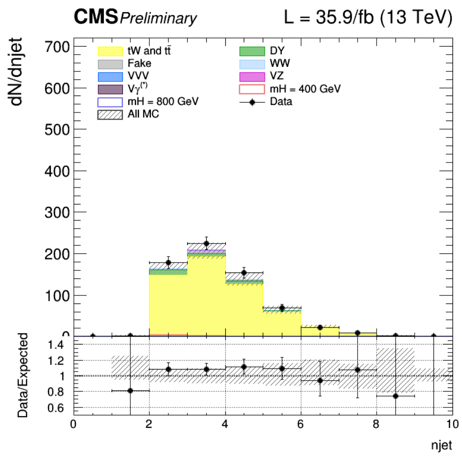

(f) $p_T^{\ell\ell}$

Figure 5.23. Control plots for several variables in a Top enriched phase space for ee.

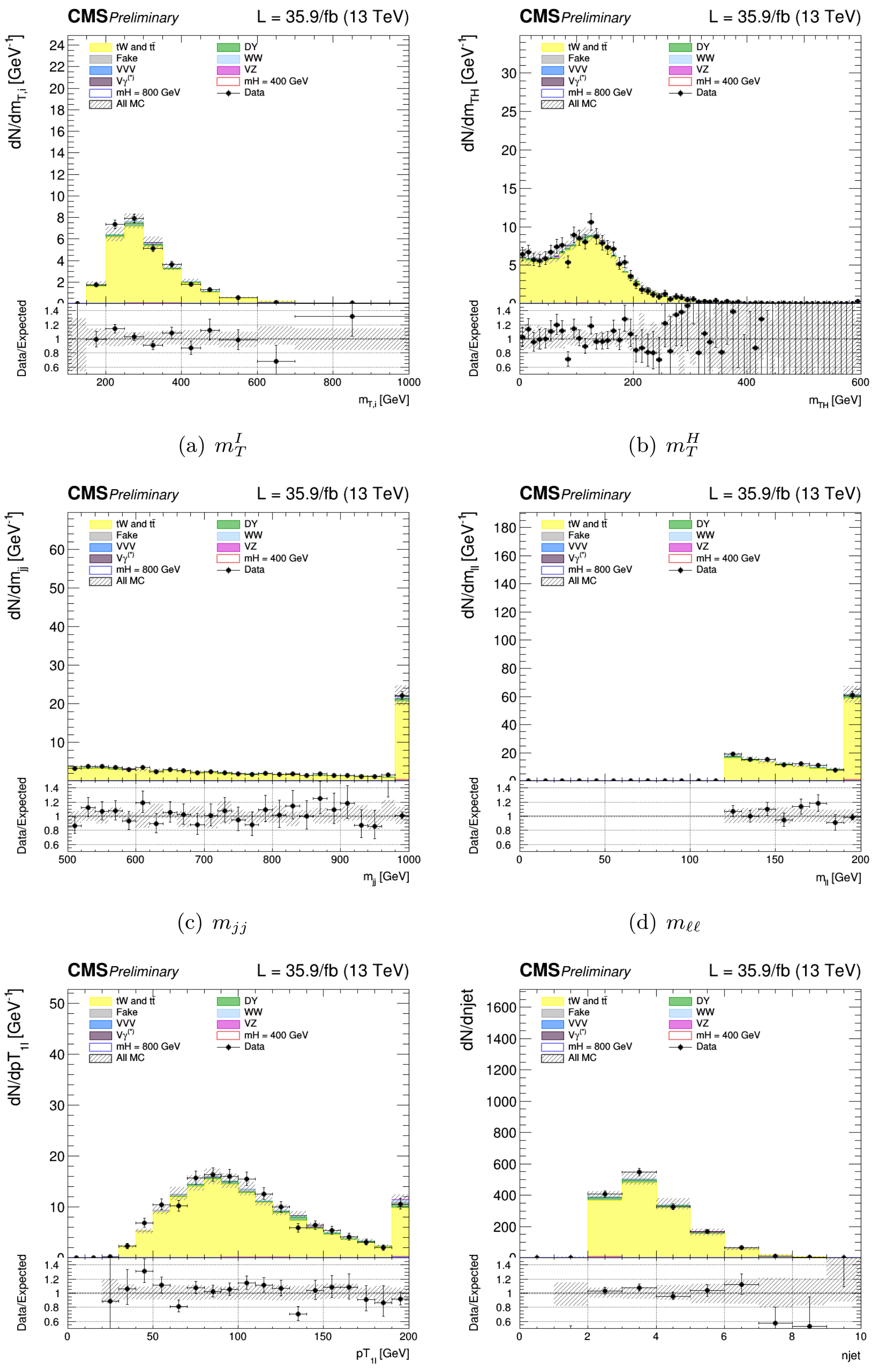

(a) m_T^I (b) m_T^H

(c) m_{jj} (d) $m_{\ell\ell}$

(e) p_T leading lepton (f) $p_T^{\ell\ell}$

Figure 5.24. Control plots for several variables in a Top enriched phase space for $\mu\mu$.

Chapter 6

Results and Interpretation

Appendix A

Special commands

Bibliography

[1] Search for high mass Higgs to WW with fully leptonic decays using 2015 data. Technical Report CMS-PAS-HIG-16-023, CERN, Geneva, 2016.

[2] HWW team. Common analysis object definitions and trigger efficiencies for the H→WW analysis with 2016 full data.

[3] SM Higgs production cross sections at $\sqrt{s} = 13\text{-}14$ TeV. `https://twiki.cern.ch/twiki/bin/view/LHCPhysics/CERNYellowReportPageAt1314TeV`.